

HUBBLE FLOWS IN THE PISCES-PERSEUS REGION FROM THE
GIOVANELLI-HAYNES GALAXY SAMPLE

T. ICHIKAWA

Kiso Observatory, Institute of Astronomy, University of Tokyo, Mitake-mura, Kiso-gun, Nagano 397-01, Japan;¹ and
Laboratory of Astronomy and Geophysics, Hitotsubashi University, Kunitachi 186, Japan

AND

M. FUKUGITA

Yukawa Institute for Theoretical Physics, Kyoto University, Kyoto 606, Japan;¹ and Institute of Astronomy,
University of Cambridge, Madingley Road, Cambridge CB3 0HA, England

Received 1991 September 26; accepted 1992 January 22

ABSTRACT

An analysis has been made of the Hubble flow for galaxies in the Pisces-Perseus supercluster region using the Tully-Fisher (TF) relation in the *B* band, applied to the sample of Giovanelli & Haynes. The number of galaxies, the depth, and the completeness of this sample offer an advantage over previous observations used in determination of the Hubble constant beyond the Virgo Cluster. Photographic surface photometry was carried out on 155 galaxies to correct for the scale error and establish the zero point of the Zwicky magnitudes, which is used in the present analysis. A large data set which contains 1119 galaxies allows us to examine various statistical errors caused by the dispersion of TF relations, observational selection effects, and an inhomogeneous spatial distribution of galaxies. We found that full control over the Malmquist bias is essential in deriving the result. The recession of galaxies is described well by a universal Hubble constant for all galaxies up to a redshift of 10,000–15,000 km s⁻¹, with the exception of those located within 2000 km s⁻¹, for which the sample is clearly affected by an inflow. The global value of the Hubble constant is $78.5_{-9.1}^{+10.3}$ km s⁻¹ Mpc⁻¹ with respect to the cosmic microwave background (CMB) rest frame or $83.2_{-9.6}^{+10.9}$ km s⁻¹ Mpc⁻¹ with respect to the Local Group centroid. In particular, for the Pisces-Perseus supercluster the Hubble constant is found to be $79.9_{-9.5}^{+10.6}$ and $86.8_{-10.1}^{+11.5}$ km s⁻¹ Mpc⁻¹, respectively. Full consistency was found with the *H*-band Tully-Fisher analysis of Aaronson and coworkers for their galaxy sample, and the difference between their value of H_0 and ours is shown to arise from the Malmquist bias. An extensive study was also made for the sources of errors. It is found that the Hubble constant derived from the Pisces-Perseus sample differs from that from the Coma Cluster; $H_0(\text{P-P})/H_0(\text{Coma}) = 0.81_{-0.10}^{+0.12}$ in the CMB rest frame. From our error analysis we conclude that this discrepancy is significant. This indicates that either the Tully-Fisher relation is not universal or the difference in recession velocity is real, all galaxies up to $\gtrsim 10,000$ km s⁻¹ moving toward the Virgo Cluster relative to the Coma galaxies or the Hubble flow being slightly anisotropic.

Subject headings: cosmology: observations — distance scale — galaxies: clustering — galaxies: distances and redshifts — galaxies: photometry

1. INTRODUCTION

The Tully-Fisher (TF) relation, a tight relationship between the luminosity of a spiral galaxy and its velocity width discovered by Tully & Fisher (1977), is generally recognized as the most promising intermediate-distance indicator. It has hitherto been applied to cluster galaxies and to galaxies in the local field by many authors to derive the Hubble constant H_0 , using optical and near-infrared wavelengths (Sandage & Tammann 1976; Mould, Aaronson, & Huchra 1980; Bottinelli et al. 1980; Aaronson et al. 1986; Bottinelli et al. 1986; Sandage 1988; Kraan-Korteweg, Cameron, & Tammann 1988, hereafter KCT; Pierce & Tully 1988; Fouqué et al. 1990; Fukugita et al. 1991). The great advantage of the TF analysis is that distances can be deduced without much resort to subjective elements. A controversy, however, remains over the value of H_0 , ranging from ~ 50 km s⁻¹ Mpc⁻¹ (Sandage 1988; KCT) to ~ 90 km s⁻¹ Mpc⁻¹ (e.g., Aaronson et al. 1986; Fukugita et al. 1991).

The distance to local calibrating galaxies was once claimed to be the main source of the uncertainty (Aaronson et al. 1986; Sandage & Tammann 1984). Nowadays, however, this uncertainty has been removed, and the accuracy of the zero point can be controlled to within 0.2 mag. Photometric data are in general not quite sufficient for clusters beyond the Virgo distance. We expect, however, the error caused by photometry to be at most 0.2 mag. A conspicuous fact is that contradictory results are sometimes derived from the same observational data. Aaronson et al. (1986) have applied the infrared TF relation to cluster galaxies in Virgo and 10 other distant clusters out to 11,000 km s⁻¹, and obtained $H_0 \approx 90$ km s⁻¹ Mpc⁻¹. They also found a bulk motion of the Local Supercluster toward the Hydra-Centaurus supercluster. KCT, on the other hand, obtained $H_0 \approx 57$ km s⁻¹ Mpc⁻¹, using the same data used by Aaronson et al., and claimed that there was no streaming motion of the Local Supercluster. This controversy arises predominantly from our lack of a proper understanding of the selection bias, in particular the Malmquist bias or its variant, the cluster population incompleteness bias, in the data: The absolute magnitude of galaxies naively averaged over a magnitude-limited sample is systematically brighter at a larger

¹ Postal address.

distance (Malmquist 1922; Teerikorpi 1987). Therefore, neglecting the effect may lead to a bias toward a higher value of H_0 , especially for distant galaxy samples.

Aaronson et al. (1986), however, argued that their samples do not suffer strongly from the bias and assumed the effect to be very small. On the contrary, KCT argued, based on their analysis for the Virgo sample, that the intrinsic dispersion of the TF relation is much larger than was thought, and the sample incompleteness bias for clusters more distant than the Virgo is very strong. KCT proposed the prescription that the true distance be obtained by fitting the observed galaxies with the curve 1–1.4 mag brighter than the central value. Unfortunately, the Virgo Cluster may have a large depth, and the obvious criticism is that the sample used by KCT is contaminated by background galaxies (e.g., van den Bergh, Pierce, & Tully 1990). We feel that neither of these two arguments is convincing, and that a proper assessment of the bias is necessary for a correct estimation of the Hubble constant.

The Malmquist bias can be estimated. For this purpose, however, we need a complete magnitude-limited sample, or at least a sample for which the completeness is known, so that the effect for galaxies not included in the sample is estimated. In practice it is also necessary that the sample size is large enough to extract a meaningful result from the analysis. There have already been a few attempts to estimate the sample incompleteness bias (Teerikorpi 1984, 1987), and these were made on cluster galaxies (Bottinelli et al. 1987). The sample that they used, however, did not satisfy the requirements, and their analysis for clusters other than the Virgo Cluster did not allow estimates of the bias.

The purpose of the present work is to estimate quantitatively the effect of the sample incompleteness bias on the determination of the cosmic distance scale both with field and cluster galaxies. In particular, we examine the effect in the Pisces-Perseus supercluster region (often referred to as the Pisces cluster region) with the H I galaxy sample provided by Giovanelli, Haynes, and their collaborators (Giovanelli & Haynes 1985, hereafter GHI; Giovanelli et al. 1986, hereafter GHMR; Giovanelli & Haynes 1989, hereafter GHII) from their survey at the Arecibo Observatory (hereafter “the Arecibo sample”). We treat the sample by clustering it into distance bins. Hence our case is virtually what is often referred to as the “cluster population incompleteness bias.” In this paper, however, we call it simply the Malmquist bias.

The great advantage of the Arecibo sample is that spiral galaxies in the Pisces-Perseus supercluster region (hereafter “the P-P region”) of $22^{\text{h}} < \alpha_{1950} < 4^{\text{h}}$, $21^{\circ}5' < \delta_{1950} < 33^{\circ}5'$ have been almost completely observed to a magnitude limit of 15.7 mag in the blue band of the Zwicky scheme (GHII). The sample contains 1119 galaxies. The survey reaches more than $100 h^{-1}$ Mpc, and the spatial distribution shows a conspicuous clustering of galaxies in the 40–50 h^{-1} Mpc region ($h = H_0/100$). The size of the sample is large enough to examine the effect of sample incompleteness. In these respects the Arecibo sample is superior to others.

However, the major disadvantage of the sample is that it lacks reliable photometric data; only the Zwicky magnitude (Zwicky et al. 1961–1968, hereafter CGCG) is available for the apparent brightness, which is crucial in determining the parameters of the TF relation. Various systematic errors have been pointed out in the Zwicky magnitude system (e.g., Sandage & Tammann 1981, hereafter RSA; Auman, Hickson, & Fahlman 1989; Bothun & Cornell 1990). We believe,

however, that this is not too fatal, if the error of the magnitude is smaller than (or comparable to) the intrinsic dispersion of the TF relation, and if the zero-point error of photometry is sufficiently controlled. In order to look into this problem, we have carried out accurate surface photometry for partial sets of the Arecibo sample using the Schmidt plates in the B band. We found that the magnitude transformation formula from m_Z to B_T proposed by Auman et al. (1989) gives sufficiently accurate B_T magnitude for our requirements; the dispersion of the magnitude error is about 0.25 mag, and the zero-point offset is 0.15 mag. The dispersion is not intolerably large, since it contributes by simply increasing the resulting dispersion of the TF relation by 20% or so. The zero-point offset can also be improved by using our photometric data directly. With these procedures we can extract fairly accurate values of the Hubble constant from both the P-P supercluster and field galaxies out to $\gtrsim 100 h^{-1}$ Mpc in the same region, with proper corrections for the sample incompleteness bias over the full distance range.

Another important point that we examine in the present analysis is the issue of large-scale streaming motions in the universe. Recently Willick (1990), with the same Arecibo sample, studied the peculiar motions of the galaxies in the P-P supercluster region using 320 spiral galaxies obtained by CCD photometry in the R band, and claimed that the great majority of objects, out to a redshift of $\sim 7000 \text{ km s}^{-1}$ have very large negative peculiar velocities streaming toward the Local Group, while the galaxies located farther away just follow the Hubble flow. In any estimation of the streaming motion it is crucial that the Malmquist bias is controlled to a sufficient accuracy; incorrect estimates of the bias easily lead to residual peculiar velocities. In the present paper we examine this problem closely and argue whether the result obtained by Willick is tenable.

It is of considerable interest to compare the present result for the Hubble constant with that from the Coma Cluster by Fukugita et al. (1991), who also made a detailed examination of the effect of the Malmquist bias, the point being that the Coma Cluster is located in a direction 90° away from the P-P region. In such a comparison, however, perhaps the most crucial factor is the calibration of photometry. We try to overcome the problem by careful Schmidt photometry of these two regions. Our analysis suggests that the value of H_0 expected from the P-P region is smaller than that from the Coma Cluster at a level of $\sim 10\%$ – 20% .

The outline of this paper is as follows. In § 2 the basic observational data of our sample are described. The observation and accurate surface photometry made with the Schmidt plates are given, and the result is compared with the existing photometric data. The problem of the errors of the Zwicky magnitude and transformation into a B_T magnitude of the RC2 scheme (de Vaucouleurs, de Vaucouleurs, & Corwin 1976, hereafter RC2) is then studied using surface photometry with sufficient accuracy. The TF relation for the galaxies in the P-P regions is obtained in § 3, and the nominal distance modulus and the Hubble ratio for each galaxy are derived in § 4: The problems of the sample incompleteness biases and some other biases arising from inhomogeneous density distribution of galaxies are discussed in great detail. Our central results are presented in § 5; the value of the corrected Hubble constant and the estimation of its uncertainty are presented. We compare our TF result with previous analyses in the literature. The issue of the bulk flow in the P-P supercluster is also discussed in this section. Finally, our conclusions are briefly summarized in § 6.

2. DATA

2.1. Arecibo Sample

We use the galaxy sample presented by Giovanelli, Haynes, and their collaborators (GHI, GHMR, GHII, hereafter collectively GH) for spiral galaxies in the region bounded by $22^{\text{h}} < \alpha_{1950} < 4^{\text{h}}$ and $21^{\circ}5 < \delta_{1950} < 33^{\circ}5$. The catalog lists a total of 1119 galaxies for which 21 cm line spectra have been detected. GHI and GHII presented a sample complete for spiral galaxies with angular diameter larger than $1'$. The full nominal completeness for spirals down to the apparent magnitude of 15.7 was achieved in their third paper (GHII). The catalog also lists some additional galaxies either taken from the *IRAS* catalog or detected serendipitously during their observations.

To make the sample magnitude-limited, we discard galaxies fainter than 15.7 mag. We also discard 13 galaxies which are listed in the CGCG under single entries but turned out to be multiple objects. This leaves 938 galaxies brighter than or as bright as 15.7 mag for our consideration. (The number of galaxies reduced by our sequential selection procedures is summarized in Table 1.)

Figure 1a shows the spatial distribution of the galaxies in the present sample, as compared with the distribution of all CGCG galaxies (Fig. 1b). It is seen that the Arecibo sample galaxies are more sparsely distributed than in the CGCG sample, in agreement with the observation that early-type galaxies are more clustered (Giovanelli & Haynes 1984). The population histogram of the CGCG (1525 galaxies) and the Arecibo sample (938 galaxies) for this region is shown in Figure 2 as a function of the Zwicky magnitude. The completeness fraction (*solid curve*) shows that it is nearly constant (about 60%–70%) irrespective of the magnitude. The incompleteness fraction of about 30%–40% is mainly due to early-type galaxies for which 21 cm line emission was not detected. In fact, the UGC (Nilson 1973) contains 68% spirals, 14% S0 + S0a,

TABLE 1

NUMBER OF GALAXIES USED IN THE PRESENT STUDY

Selections of the Sample	Number
Giovanelli-Haynes sample	
(all galaxies with H I data)	1119
Zwicky galaxies ($m_z \leq 15.7$) selected	951
Double system excluded	938
Galaxies with morphological peculiarity/confused	
H I data excluded	881
Morphology Sa-S/Irr ($T = 3-8$ in GH) selected	636
$i \geq 45^\circ$ selected	461
$V_c = 2000-15,000 \text{ km s}^{-1}$	
and $\log \Delta v = 2.35-2.75$ selected	393

8% E + E/S0 and other galaxies in this strip, which are close to the "field" value S:S0:E = 65%–70%:23%–15%:12%–14% (Postman & Geller 1984). Therefore, we consider that the Arecibo survey is nearly complete for spiral galaxies to 15.7 mag.

We will use the morphological type classification (T) given in the Arecibo catalog. The spiral galaxies of unspecified morphology (e.g., "S..." in the UGC) are given $T = 5$.

The H I recession velocities with respect to the velocity centroid of the Local Group with the standard IAU correction $300 \sin l \cos b$ (Haynes & Giovanelli 1984) are further transformed, when necessary, into the value in the cosmic microwave background (CMB) rest frame using the dipole of $V_c = 622 \text{ km s}^{-1}$ toward the apex of ($l = 277^\circ$, $b = 30^\circ$) (Smoot et al. 1991).

2.2. Surface Photometry for Sample Galaxies

Haynes & Giovanelli (1984) adopted Zwicky magnitudes for the Arecibo sample, correcting for the systematic scale errors of

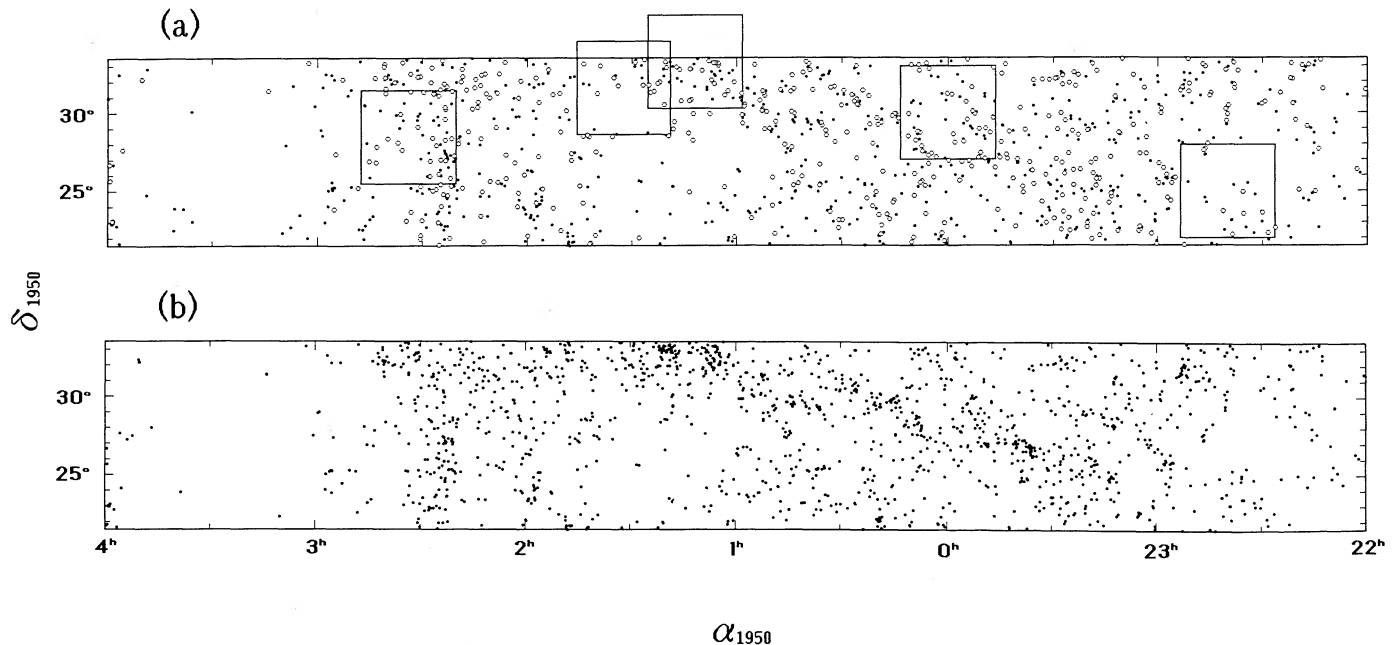


FIG. 1.—(a) Spatial distribution of galaxies in the Arecibo sample on the sky. The open circles represent the 461 galaxies with Sa-Sc/Irr morphological types and with inclination greater than 45° used to obtain the Hubble constant. The fields enclosed by boxes show the regions for which photographic surface photometry was done. (b) Spatial distribution of all galaxies in the CGCG for comparison.

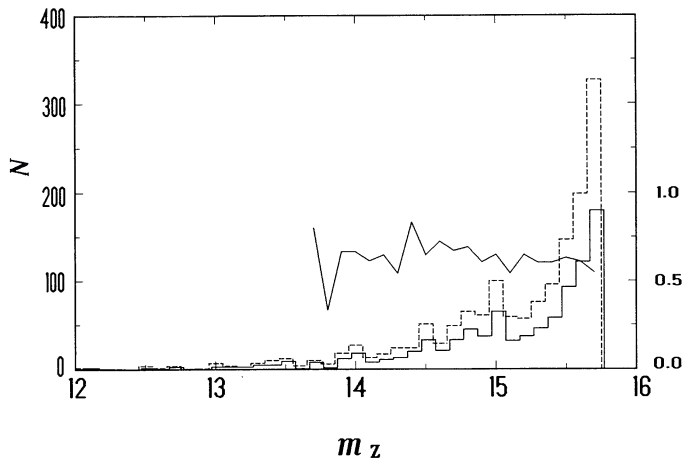


FIG. 2.—Number of galaxies in the Arecibo sample as a function of Zwicky magnitude (solid-line histogram), as compared with all galaxies in the CGCG (dashed-line histogram). The fraction of galaxies in the Arecibo sample to those in the CGCG is also shown by a solid curve.

the CGCG according to Kron & Shane (1976). The Zwicky magnitudes suffer from systematic errors as large as 0.3–0.5 mag, or worse, close to the faint end. In order to correct errors to a tolerable level, we performed surface photometry of some sample galaxies on the photographic plates (Kodak 103a-O or IIa-O plates plus Schott GG 385 filter) taken with the 105 cm Schmidt telescope at the Kiso Observatory (plate numbers K2975, K3395, K3397, K5254, and K6452). The fields are shown by boxes in Figure 1a. All galaxies in the Arecibo sample (155 galaxies) in those fields were scanned by the PDS 2020GMS microdensitometer at the Kiso Observatory. The analysis of the scanned data was made by the Kwasan Image Processing System at the Kwasan Observatory and cross-checked by the image processing system at the Kiso Observatory.² Zero points are calibrated by the photoelectric aperture magnitudes compiled by Longo & de Vaucouleurs (1983, hereafter LdV) (93 data points for 27 galaxies). The sky surface brightness obtained from these calibrators agrees to within

² We thank S. Okamura for kindly checking our result with the image processing system at the Kiso Observatory.

0.14 mag (1σ) for a single plate and varies from 21.8 to 22.7 mag arcsec⁻² in five fields.

After subtracting the sky brightness, we measured the intensity of galaxies on circular annuli outward from the galaxy center with 1 pixel interval, and a growth curve is thus obtained for each galaxy by an aperture photometry program after removing stars. The morphology-dependent template curves given by de Vaucouleurs (1977) were adjusted to our growth curves by a sliding fit to derive total magnitudes B_T defined in RC2. Since the present photometry is based on Schmidt plates with a small image scale (62"5 mm⁻¹), the very central region [$\log(A/D_{25}) < -0.7$] was not used in the fitting. The faint outer region [$\log(A/D_{25}) > -0.2$] was also assigned a lower weight to avoid the effect of noise and a possible slight error in the sky subtraction.

The external error of our photometry was investigated by comparing our magnitudes with those in the literature (see Table 2). We first made a comparison with B_T listed in RC2. In our five fields, there are 19 galaxies with B_T magnitudes available in RC2. We found that $B_T(\text{RC2}) - B_T(\text{Kiso}) = +0.01$ mag with a standard deviation $\sigma = 0.15$ mag (Fig. 3). The dispersion is primarily caused by errors in the zero-point calibration using photoelectric aperture photometry. No systematic difference is detected between our total magnitudes and those in RC2.

Further comparison is made with the photometry by Bothun et al. (1985) and by Cornell et al. (1987). The former has often been used in the TF analysis by several authors (e.g., Bottinelli et al. 1987; KCT). Comparing 28 aperture magnitudes of Bothun et al. with ours for 18 common galaxies, we found that the zero point of Bothun et al. is 0.09 mag fainter than ours, which is established by the zero point of LdV. (We note here that the same trend was also observed for Coma Cluster galaxies by Fukugita et al. 1991.)

For B_T we obtained³ $B_T(\text{Bothun et al.}) = B_T(\text{this work}) + 0.21$ with $\sigma = 0.36$. The discrepancy in B_T is larger than 0.8 mag for a few cases (NGC 582, UGC 669). A part of this large offset may be due to the fact that Bothun et al. used a common growth curve for all of the galaxies and enhancement of errors from the growth curve fitting procedure of aperture magnitude, especially for faint galaxies. Let us also note that one-third of

³ We calculated B_T from B_T^0 given by Bothun et al. according to the prescription given in their paper.

TABLE 2
COMPARISON OF THE ZERO POINT OF PHOTOMETRY AND THE TOTAL MAGNITUDE

REFERENCE	APERTURE MAGNITUDE				TOTAL MAGNITUDE		
	n	n'	$m(\text{ref}) - m(\text{Kiso})$	σ	n	$B_T(\text{ref}) - B_T(\text{Kiso})$	σ
Pisces-Perseus							
RC2/LdV	27	93	0 ^a	0.14	19	+0.01	0.15
Bothun et al. 1985	18	28	+0.09	0.16	13	+0.21	0.36
Cornell et al. 1987	6	6 ^b	+0.01	0.18
Coma (Fukugita et al. 1991)							
RC2/LdV	13	128	0 ^a	0.08	12	-0.03	0.16
Bothun et al. 1985	26	87	+0.13	0.11	25	+0.23	0.24
Cornell et al. 1987	7	7	+0.17	0.07

NOTE.— n = number of galaxies; n' = number of data points.

^a Zero-point calibration.

^b UGC 1045 is excluded.

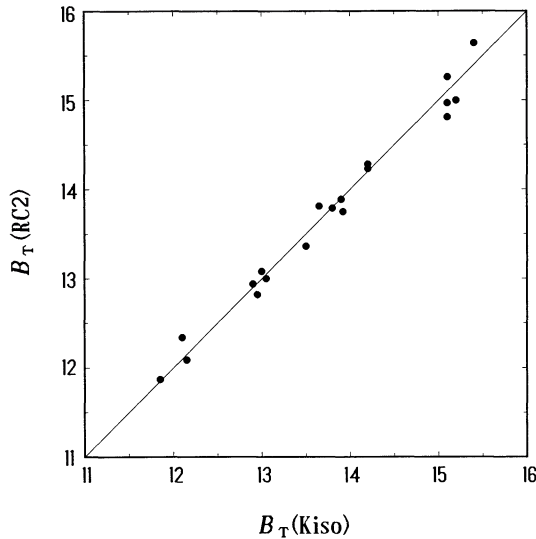


FIG. 3.—Comparison of our B_T magnitudes measured on the Kiso Schmidt plates with those given in RC2.

the B_T values obtained by Bothun et al. are based on magnitudes measured at one aperture.

Finally, we compared our aperture magnitudes at 25 mag arcsec⁻² with those of CCD photometry by Cornell et al. (1987) for seven galaxies. We found that the agreement is quite satisfactory: $B_{25}(\text{Cornell et al.}) = B_{25}(\text{this work}) + 0.01$ with $\sigma = 0.18$. Here we excluded UGC 1045, for which two photometries gave very discrepant answers ($\Delta B_{25} = -0.56$ mag).

It is sometimes claimed that photographic photometry is less accurate than that based on CCD because of nonlinearity of the photographic emulsion. We feel, however, that well-calibrated photographic photometry is accurate enough to

evaluate the total magnitude of galaxies within an error of 0.1 mag at least to around 15 mag (e.g., Fukugita et al. 1991), which is sufficiently accurate for our purpose.

Our surface photometry will be published elsewhere.

2.3. Calibration of the Zwicky Magnitude

Schmidt plates archived at the Kiso Observatory do not cover the strip surveyed by Giovanelli and Haynes. Therefore, we use the Zwicky magnitude corrected for its scale errors. In Figure 4a we compare m_Z with B_T in the present region and see large scatter, especially near the faint end. There are a few works on correcting the scale error of the Zwicky magnitude (for reviews see Fasano 1985; Bothun & Cornell 1990). The most elaborate among them is the transformation by Auman et al. (1989) into the B_T magnitude of RC2. They gave the formula

$$m_Z^c(\text{AHF}) = 0.989m_Z - 0.357S_B + 8.41, \quad (1)$$

where S_B is the surface brightness defined as $S_B = m_Z + 2.5 \log(ab) + 8.63$, and a and b are blue major and minor axes of the galaxy in arcminutes given in the UGC. We examine the accuracy of this formula using photometry of 103 galaxies obtained in § 2.2 and another 16 galaxies of RC2 in the present Arcicibo strip not covered by our photometry. We show in Figure 4b the magnitude transformed by equation (1). Here we are limited to galaxies brighter than or as bright as 15.7 mag in m_Z , and exclude those for which accurate surface photometry is not obtained owing to confusion by stars or other galaxies. The apparent nonlinearity in the Zwicky magnitude is substantially corrected, and the dispersion around the regression line decreases from 0.31 to 0.26. The regression line of Figure 4b is

$$m_Z^c(\text{AHF}) = B_T + 0.15 \quad (\sigma = 0.26). \quad (2)$$

This is already at a tolerable level for our work, because the zero-point offset is only 0.15 mag and the dispersion of photometry errors is now smaller than that expected from the

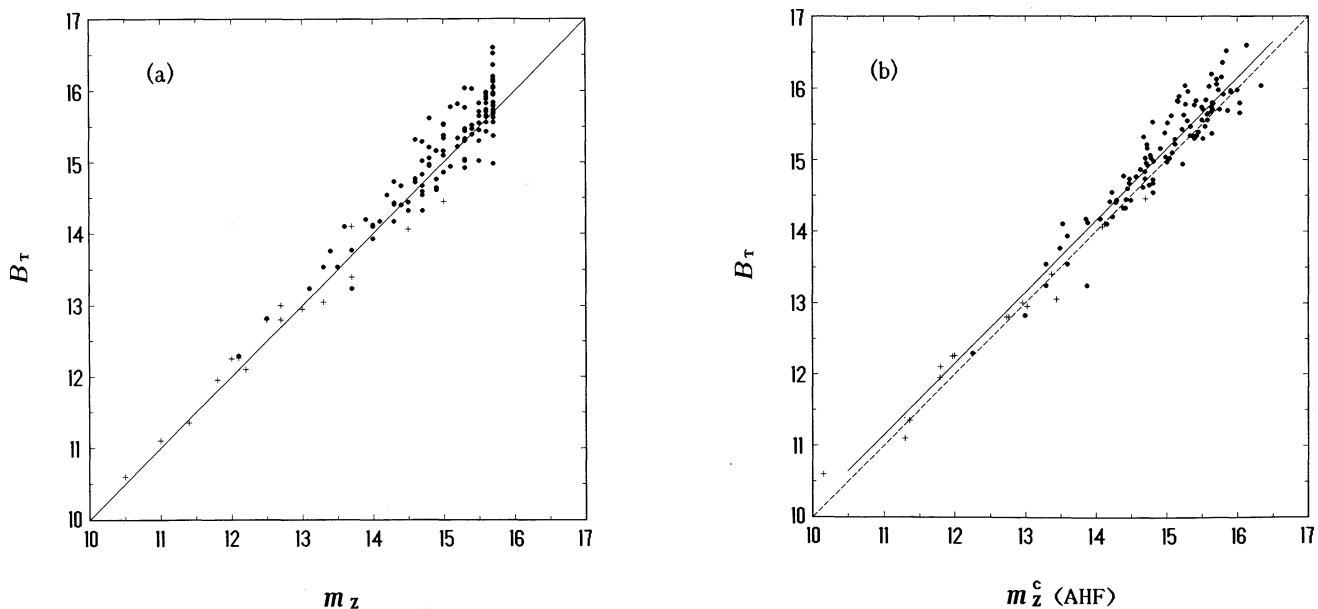


FIG. 4.—(a) Comparison of total magnitudes $B_T(\text{Kiso})$ of Arcicibo galaxies defined by the RC2 scheme with Zwicky magnitudes for 103 galaxies (filled circles) and 16 galaxies quoted from RC2 in the present strip region with Zwicky magnitudes (plus signs). (b) Comparison of B_T and corrected Zwicky magnitudes with the aid of the formula of Auman et al. (1989).

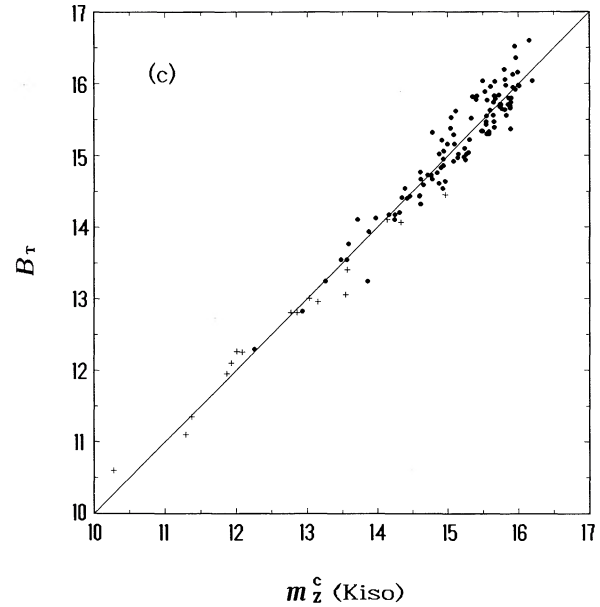
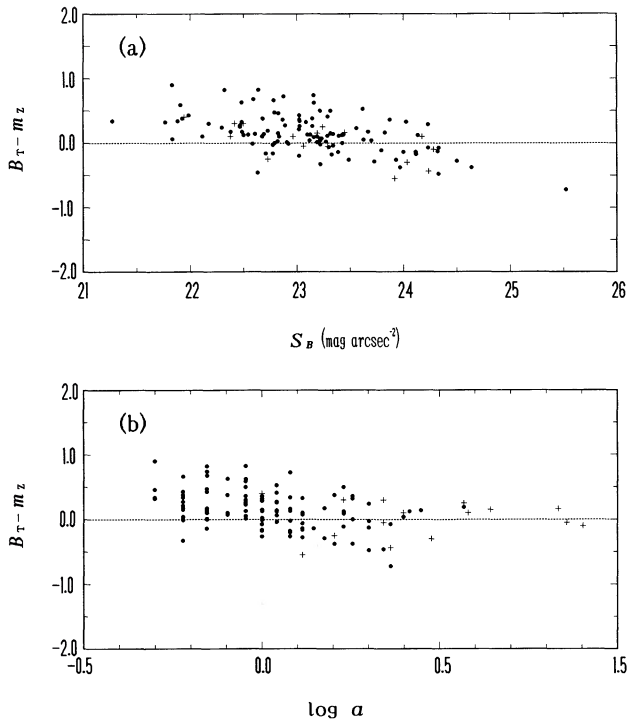


FIG. 5.—Dependence of $B_T - m_z$ (a) on surface brightness S_B and (b) on the size of the major-axis diameter a . (c) Comparison of total magnitudes B_T in the RC2 scheme to corrected Zwicky magnitudes with the aid of eq. (3). Plus signs show the galaxies quoted from RC2.

intrinsic scatter of the TF relation ($\sigma_{TF} \sim 0.4$ mag); the photometry error increases the net dispersion by only 20%.

In order to explore the possibility of improving the transformation further, we plot in Figure 5 the correlation of $B_T - m_z$ with the major-axis size of the galaxies (Fig. 5b) as well as with surface brightness (Fig. 5a). The correlation with surface brightness was taken into account by Auman et al., who showed that the Zwicky magnitude is brighter for galaxies with a high surface brightness. In Figure 5b we also see that m_z is brighter for galaxies with a small size. In addition, we note that most of the Zwicky magnitudes for the galaxies with a size smaller than $1'$ are estimated to be brighter than the true value by 0.5 mag. Taking this observation into account, we obtain a conversion formula that might be more suitable for galaxies in the strip we are concerned with:

$$m_z^c = 0.921m_z - 0.158S_B - 0.504 \log a + 4.99, \quad (3)$$

with a standard deviation of $\sigma = 0.24$ mag (Fig. 5c). We consider that the new formula is better than or at least as good as equation (1) in this region, and it at least improves the zero-point offset. We may quote 0.1–0.15 mag as the error of the zero-point of the corrected Zwicky magnitude. We expect that the net dispersion of the errors of photometry is about $[(0.1)^2 + (0.24)^2]^{1/2} \approx 0.26$ mag. In the following we use m_z^c given by equation (3) as B_T .

2.4. Inclination

To evaluate the TF relation, we need the velocity width to be corrected for the inclination i and for redshift effect into an edge-on value at the rest frame. For this purpose we adopt the simplest prescription used by Aaronson, Mould, & Huchra (1980),

$$\Delta v^c = \Delta V_{20}/(1+z) \sin i. \quad (4)$$

We obtain the inclination i of a galaxy from the conventional formula given by Hubble (1926) for oblate spheroids,

$$\cos^2 i = \frac{q^2 - q_0^2}{1 - q_0^2}, \quad (5)$$

with $q = b/a$ and $q_0 = c/a$, where a , b , and c are three axes of the spheroid. In agreement with the prescription given by Aaronson et al. (1980), we fix q_0 to 0.2 and add to i derived from this formula the value $\Delta i = 3^\circ$. The Arecibo catalog uses the values of $q_0 = 0.10$ –0.23, depending on morphological types of galaxies (Haynes & Giovanelli 1984). The value derived in this way leads to at most a 2% difference in $(\sin i)^{-1}$ compared with that obtained with $q_0 = 0.2$. In spite of the fact that the small change in q_0 or i will have no serious effect on the result, we adopt the $\Delta i = 3^\circ$ prescription of Aaronson et al. (1980) to make the definition consistent with those used for local calibrators.

We found errors in b/a to be much more important. An inclination cut $i > 45^\circ$ or $i > 30^\circ$ is usually imposed in the literature. This is necessary not only to avoid a large, unwanted correction to the line-width velocity but also to reduce the error arising from the uncertainty of b/a . For example a 10% error in b/a leads to a 11% error in $(\sin i)^{-1}$ for $i = 45^\circ$, but it causes a 26% error if $i = 35^\circ$. We choose the cutoff $i \geq 45^\circ$. This cutoff, together with the selection of the morphology types Sa–S/Irr ($T = 3$ –8 in GH), leaves 461 galaxies for the TF analysis.

Let us now transform the axis ratios listed in the Arecibo catalog, which come mainly from the UGC or their own measurement on the POSS glass copies (Haynes & Giovanelli 1984; GHI; GHMR; GHII), into R_{25} of RC2. The sizes of galaxies measured by our photometry are compared with those by CCD photometry of Cornell et al. (1987), and no systematic errors are detected in our major axis and axial ratios. The

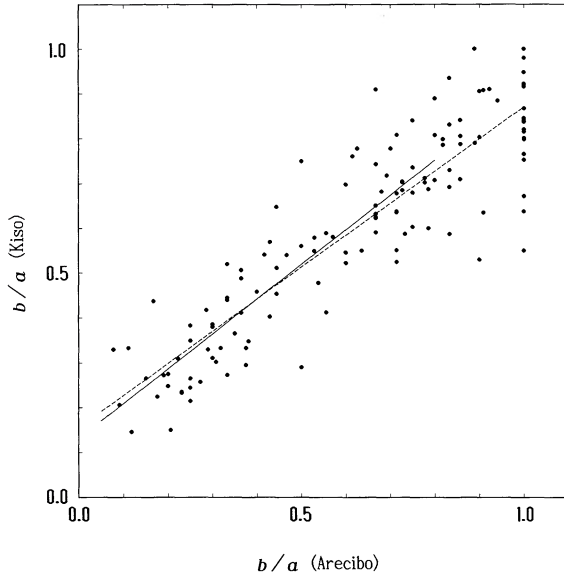


FIG. 6.—Comparison of the axial ratios b/a in the Arcicibo catalog with those of the isophote at $25 \text{ mag arcsec}^{-2}$ measured in the present surface photometry. The solid line shows the regression for the galaxies with $b/a < 0.8$ which corresponds to inclination $i > 45^\circ$. The dashed line shows the regression for all galaxies in the figure.

differences in a and b/a are $+0.003$ ($\sigma = 0.158$) and $+0.003$ ($\sigma = 0.053$), respectively. We compare in Figure 6 axial ratios b/a at $25 \text{ mag arcsec}^{-1}$ measured on the Kiso Schmidt plates with those in the Arcicibo catalog for the 133 galaxies. The regression line for $i > 45^\circ$ [$(b/a)_{\text{Arcicibo}} < 0.80$] is given by

$$(b/a)_{\text{Kiso}} = 0.78(\pm 0.04)(b/a)_{\text{Arcicibo}} + 0.13(\pm 0.02), \quad (6)$$

with a dispersion of $\sigma = 0.09$. The uncertainty of $(\sin i)^{-1}$ corresponding to this dispersion is 16% for $i = 45^\circ$ and 8% for $\langle (\sin i)^{-1} \rangle$ for a uniform distribution of the galaxies.

2.5. Velocity Width Data

The 21 cm line widths given in the Arcicibo catalog use a definition somewhat different from that conventionally used for the TF analysis; the Arcicibo catalog presents W_1 and W_2 , given as the width at 50% of the mean profile and 50% of the peak intensity of 21 cm line emission, respectively, whereas TF work customarily uses the velocity widths defined at the 20% level of the peak intensity, ΔV_{20} , as in e.g., Aaronson et al. (1982). The local calibration that we are going to use also adopts this definition (Fukugita et al. 1991). Haynes & Giovanelli (1984) suggested a conversion formula $\Delta V_{20} = W_1 + 12 \text{ km s}^{-1}$. By comparing W_1 with ΔV_{20} given by Aaronson et al. (1980, 1982) and Bothun et al. (1985) for 35 galaxies common to two samples (Fig. 7), we obtained $\Delta V_{20} = W_1 + 12.7 \text{ km s}^{-1}$ ($\sigma = 17.4 \text{ km s}^{-1}$), in agreement with Haynes & Giovanelli (1984). We then calculate edge-on velocity widths corrected for inclination and redshift effect according to

$$\Delta v^c = (W_1 + 12.7)/(1 + z) \sin i. \quad (7)$$

In Figure 8 we show the histogram for the distribution of corrected line widths. At first sight we see that there are fewer galaxies with line width $\log \Delta v^c < 2.38$. We must now ask whether this is not due to undersampling of galaxies with small H I line width. For this purpose we calculate model distribu-

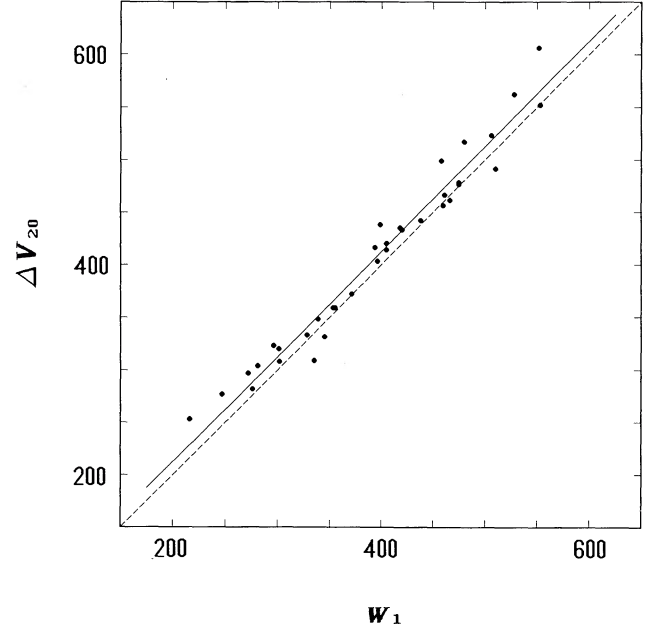


FIG. 7.—Comparison of two 21 cm H I line widths with different definitions. W_1 and ΔV_{20} stand for velocity widths at a 50% level of the mean profile (Haynes & Giovanelli 1984) and at a 20% level of the peak intensity (Aaronson et al. 1980), respectively. The regression line $\Delta V_{20} = W_1 + 12.7 \text{ km s}^{-1}$ is shown by a solid line.

tions of the line width using the luminosity function (see eq. [8] below) and a model line-width distribution for a given luminosity (see eq. [14] below). In fact, if the spatial distribution of galaxies was uniform (*dashed curve*), we should have more galaxies with small H I line width. If a realistic spatial distribution (Fig. 10; see Fukugita & Ichikawa 1992 for details) is used

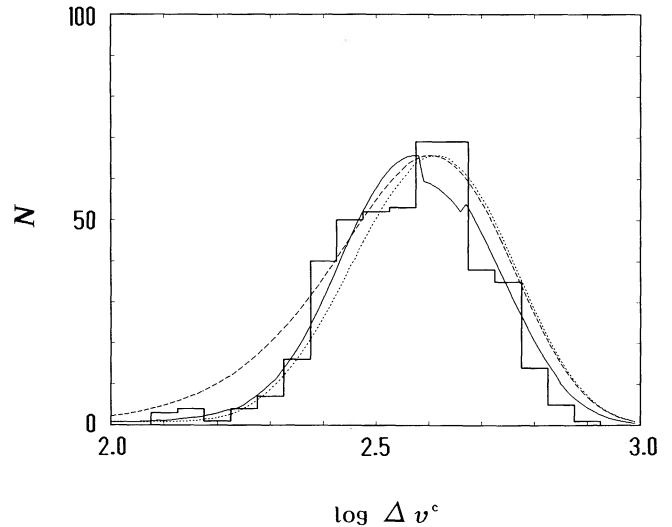


FIG. 8.—Distribution of the 21 cm line width at a 20% level corrected for inclination and redshift. A selection is made for $i \geq 45^\circ$. The dashed curve shows the expected number of galaxies assuming a spatially uniform distribution with no selection bias in the H I observation. The solid curve is the prediction for the observed galaxy distribution (see Fig. 10 below). The dotted curve is for a simplified model in which no galaxies are assumed in the $V_c = 2000\text{--}4000 \text{ km s}^{-1}$ region, to show the cause for the deficiency of low line width galaxies.

(solid curve), however, the model curve reproduces the data very well, including the slight deficiency of galaxies with large line width. In particular, a lack of galaxies with small H I line width is ascribed to a lack of galaxies in the 20–40 h^{-1} Mpc region. The dotted curve obtained using a model density distribution with a void in the 20–40 h^{-1} Mpc region explicitly demonstrates this. Therefore, it is concluded that a somewhat odd shape of the line-width distribution does not represent any selection bias in the H I observation.

2.6. Absorption Corrections

2.6.1. Galactic Absorption, A_B

The P-P region is located rather close to the Galactic plane (Galactic latitude $b = -40^\circ$ to -16°). The Galactic absorption is patchy and varies much from place to place, with a gradual increase toward the east. Toward its eastern end, the P-P supercluster becomes obscured by the Perseus dark clouds. Therefore, a careful correction for Galactic absorption for each galaxy is important. Haynes & Giovanelli (1984) used the absorption correction given by Burstein & Heiles (1978, 1982, 1984, hereafter collectively BH) based on the H I column density and galaxy counts. The absorption correction formula given in RC2 also reproduces this patchy cloud distribution well. If we adopt the RC2 scheme, we obtain $\langle A_B(\text{RC2}) - A_B(\text{BH}) \rangle = 0.12$ mag, and the dispersion is 0.09 mag. The difference is mostly ascribed to the zero-point offset at the Galactic polar caps. The correction of Galactic absorption by a smooth cosecant law as in RSA is not applicable in the present low Galactic latitude. (The RSA formula gives an absorption correction still 0.08 mag smaller than that of BH.)

We take the absorption correction scheme consistently for both the galaxies in the P-P region and local calibrators. Table 3 summarizes A_B averaged over galaxies for various schemes. In this table we see that the difference between A_B for galaxies in the P-P region and for those of local calibrators does not differ more than 0.04 mag from scheme to scheme. The circumstantial evidence that these absorption corrections are not in serious error (at least relative to those for local calibrators) will be discussed in § 5.7.

2.6.2. Internal Absorption, A_i

The RC2 scheme and the RSA scheme are two alternatives widely employed to correct for internal absorption. The RSA scheme gives a larger absorption correction, and it may differ from that of RC2 by as much as 0.7 mag for early-type (Sa–Sb) spirals. This large correction often causes a wider scatter of the Tully-Fisher plot. Nevertheless, we use both schemes and compare the results in order to examine the model dependence. The model dependence cancels out to a large extent between the Pisces-Perseus galaxies and the local calibrators, and the net difference between the two schemes is 0.13 mag (this makes the RSA distance 6% smaller).

TABLE 3

AVERAGE ABSORPTION CORRECTIONS

REFERENCE	ARECIBO SAMPLE		LOCAL CALIBRATORS	
	$\langle A_B \rangle$	$\langle A_i \rangle$	$\langle A_B \rangle$	$\langle A_i \rangle$
RC2	0.33	0.27	0.28	0.23
BH	0.21	...	0.12	...
RSA	0.13	0.76	0.07	0.59

2.6.3. K-Correction, K_B

For the K-correction, we take the linear correction of RC2.

2.6.4. Total Corrected Magnitude

The corrected magnitude is given by $B_T^0 = B_T - A_B - A_i - K_B$ if the RC2 scheme is used, and B_T is identified with m_z^c of equation (3). The corrected magnitude is denoted as $B_T^{0,i}$ if the RSA scheme is used.

2.7. Selection Functions

Selection functions play a central role in our work to estimate the effect of the Malmquist bias on distance estimates. In order to estimate selection functions, we need knowledge of the density distribution and the luminosity function. Since the estimate of density distributions requires selection functions, we have to determine both quantities in a self-consistent way. The expected number of galaxies as a function of magnitude however, depends very weakly on details of the density distribution, and the iteration procedure converges quite rapidly. We assume that the luminosity function is universal and take it to be of the Schechter form (Schechter 1976),

$$\phi(L)dL = \phi^*(r)(L/L^*)^\alpha e^{-L/L^*} dL/L^*, \quad (8)$$

where L^* is chosen to be a value corresponding to $M^* = -19.22 + 5 \log h$ (corrected for the internal absorption of 0.24 mag with $h = 0.75$ and $\alpha = -1.16$ as given by Efstathiou, Ellis, & Peterson 1988 for Sb–Sc galaxies). The result is insensitive to the choice of parameters for observationally allowed ranges.

In Figure 9 the population histogram is shown for the 938 galaxies as a function of $m_0 \equiv B_T^0$. By comparing it with a curve $N(m_0) \propto 10^{0.6m_0}$ normalized to the histogram at brighter magnitude ($B_T^0 \leq 15.1$ mag), we obtain a trial selection function. The density distribution (integrated over right ascension and declination) is then estimated as a function of the distance using the trial selection function and the luminosity function. We then predict $N(m_0)$. This procedure is iterated. In Figure 9

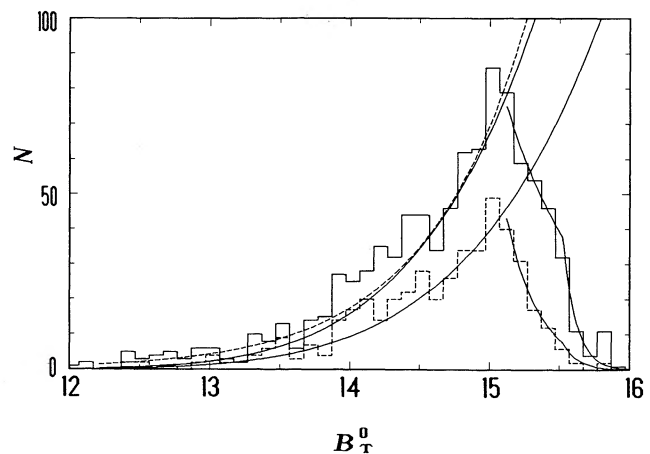


FIG. 9.—Distribution of 938 galaxies as a function of B_T^0 magnitude corrected for Galactic and internal absorptions and with the K-correction using the RC2 scheme. The solid curve shows the distribution expected from the galaxy distribution of Fig. 10. The dotted curve indicates $N \propto 10^{0.6B_T^0}$. The histogram with dashed lines represents the 461 galaxies with Sa–Sc/Irr morphological types and inclination greater than 45° used for our TF analysis. The solid curve below ($B_T^0 \leq 15.1$ mag) is obtained by scaling the solid curve for the full sample. The solid curve for $B_T^0 > 15.1$ mag is a fit to the observed distribution which yields the selection function (9).

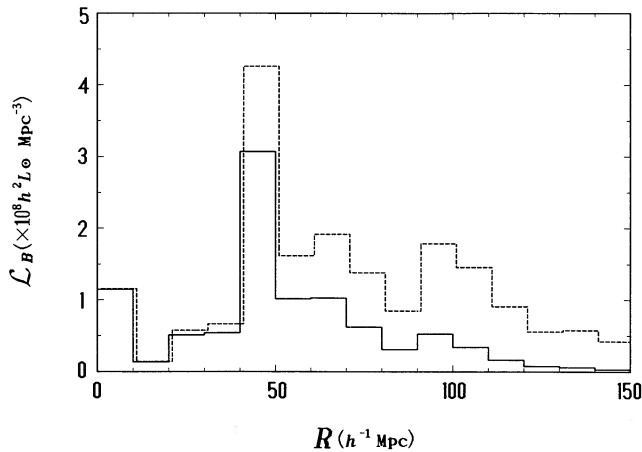


FIG. 10.—Luminosity density distribution for Sa-Sc/Irr galaxies as a function of the distance defined by the recession velocity averaged over the declination and right ascension in the strip. The solid curve shows the distribution corresponding to the observed galaxies, and the dashed curve shows the true luminosity distribution estimated with the use of the luminosity function and the selection function discussed in the text.

we show $N(m_0)$ thus obtained by a solid curve. The resulting curve differs from the initial $10^{0.6m_0}$ curve only slightly. This means that one iteration suffices to obtain the selection function and the density distribution. Another histogram shown in Figure 9 is a population distribution with the 461 galaxies used in our final analysis. The selection function obtained for the 461 galaxies is

$$f(m_0) = \begin{cases} 1 & \text{for } m_0 \leq 15.1, \\ 10^{-2.43(m_0 - 15.1)} & \text{for } 15.1 < m_0 \leq 15.4, \\ 10^{-4.50(m_0 - 15.4) - 0.73} & \text{for } 15.4 < m_0 \leq 16.0, \\ 0 & \text{for } m_0 > 16.0, \end{cases} \quad (9)$$

with $m_0 = B_T^0$.

We present in Figure 10 the density distribution as a function of distance (see Fukugita & Ichikawa 1992 for more details). We observe conspicuous large-scale inhomogeneities. A strong concentration of galaxies around $50 h^{-1}$ Mpc corresponds to the P-P supercluster. The fact that the density in the foreground ($R \sim 20\text{--}40 h^{-1}$ Mpc) is much smaller than the average value ($\mathcal{L}_B \sim 1.3 \times 10^8 h^2 L_\odot \text{Mpc}^{-3}$) indicates the presence of a void.

3. TULLY-FISHER RELATIONS

3.1. Local Calibrator

We adopt the zero point of the TF relation given by Fukugita et al. (1991), who basically employed distances to local calibrators given in a review by Tammann (1987) and slightly updated them to include several new studies for the distance moduli to nearby galaxies made after Tammann's review. The calibration is based on the distance to the eight local calibrators of Tammann (1987) and KCT. Four calibrators (M31, M33, NGC 300, and NGC 2403) have the distance determined well by Cepheid variables. The distance to M81 was revised as much as 1.1 mag from 1974 to 1987 (Tammann 1987) and is now given a value close to the original 1974 value from the Cepheid measurement of Freedman (1990) and the planetary

nebula luminosity function work of Jacoby et al. (1989). The distances to NGC 247, NGC 253, and NGC 7703 are estimated only through resolution into bright stars (Sandage & Tammann 1984). Fukugita et al. (1991) carried out a chi-square fitting with an appropriate weight put on these data to derive the TF relation of the local calibrators, instead of a least-squares fitting with an equal weight assigned to all local calibrators. We take as a reference choice their fit I with the absorption correction method of the RC2 scheme:

$$M_{B_T^0} = -19.12(\pm 0.16) - 6.35(\pm 0.86)(\log \Delta v^c - 2.5). \quad (10)$$

The calibrators are distributed over a range of line widths $\log \Delta v^c = 2.36\text{--}2.75$. The scatter of the points around the fit is about $\sigma = 0.4$ mag. The adoption of Freedman's (1990) Cepheid distance (fit V of Fukugita et al.) makes the calibration curve 0.08 mag brighter. For the Tully-Fisher relation with the RSA scheme we take fit III.

3.2. Tully-Fisher Relations in the Pisces-Perseus Region

We determine the parameters of the TF relation for the galaxies for the recession velocity intervals of 2000 km s^{-1} in the P-P region. We take galaxies of morphological types Sa-S/Irr and $i \geq 45^\circ$. Galaxies showing morphological peculiarity or with confused H I profiles are excluded. The result is shown in Figure 11 for the 461 galaxies, where the absolute magnitudes are derived using the Hubble distance with the normalized Hubble constant h ($h = H_0/100$) in the CMB rest frame and the absorption correction of the RC2 scheme.

Sa and Sab galaxies are distinguished from later types by different symbols (*crosses*) to examine the morphological segregation in the TF relation. Sixteen out of the 20 Pisces galaxies considered by Aaronson et al. (1986) are contained in our sample (two are outside the region and another two are fainter than our limiting magnitude) in the bin of $4000\text{--}6000 \text{ km s}^{-1}$ and denoted by open circles. Least-squares fits of the form

$$-M_{B_T^0} = A + B(\log \Delta v^c - 2.5) + 5 \log h \quad (11)$$

are applied to galaxies in each velocity bin either leaving the slope B as a free parameter (fit [i]) or setting B equal to the value of the local calibrators (fit [ii]). We also tried the prescription proposed by Schechter (1980), fitting $p = \log \Delta v^c$ as a function of $M_{B_T^0}$ (fit [iii]):

$$\log \Delta v^c - 2.5 = -(5 \log h + A)/B - M_{B_T^0}/B. \quad (12)$$

The results are given in Table 4. In the second column n is the number of galaxies in each velocity bin used for the fit.

A noteworthy point, apparent in Figure 11 and Table 4, is that the slope parameter B of fit (i), which is consistent with the value of equation (10) for the $2000\text{--}4000 \text{ km s}^{-1}$ sample, decreases as the distance of the sample increases. This is evidence for the existence of Malmquist bias typical of a magnitude-limited sample in which intrinsically faint galaxies are missing at the distant end. Therefore, the Hubble constant (col. [8] in Table 4) nominally obtained by fixing the slope parameter to the local calibrator value (fit [ii]) and equating $-M_{B_T^0}$ of the Pisces-Perseus galaxies to the left-hand side of equation (10) suffers from this bias, as is also clear from the increase of h with increasing distance. This means that a proper correction for the bias is essential in obtaining the true value of the Hubble constant from the present galaxy sample.

It has been noted by Schechter (1980) that the Malmquist bias can be avoided if the data points are fitted for $\log \Delta v^c$ as a function of $M_{B_T^0}$ (fit [iii]), provided that the H I line-width

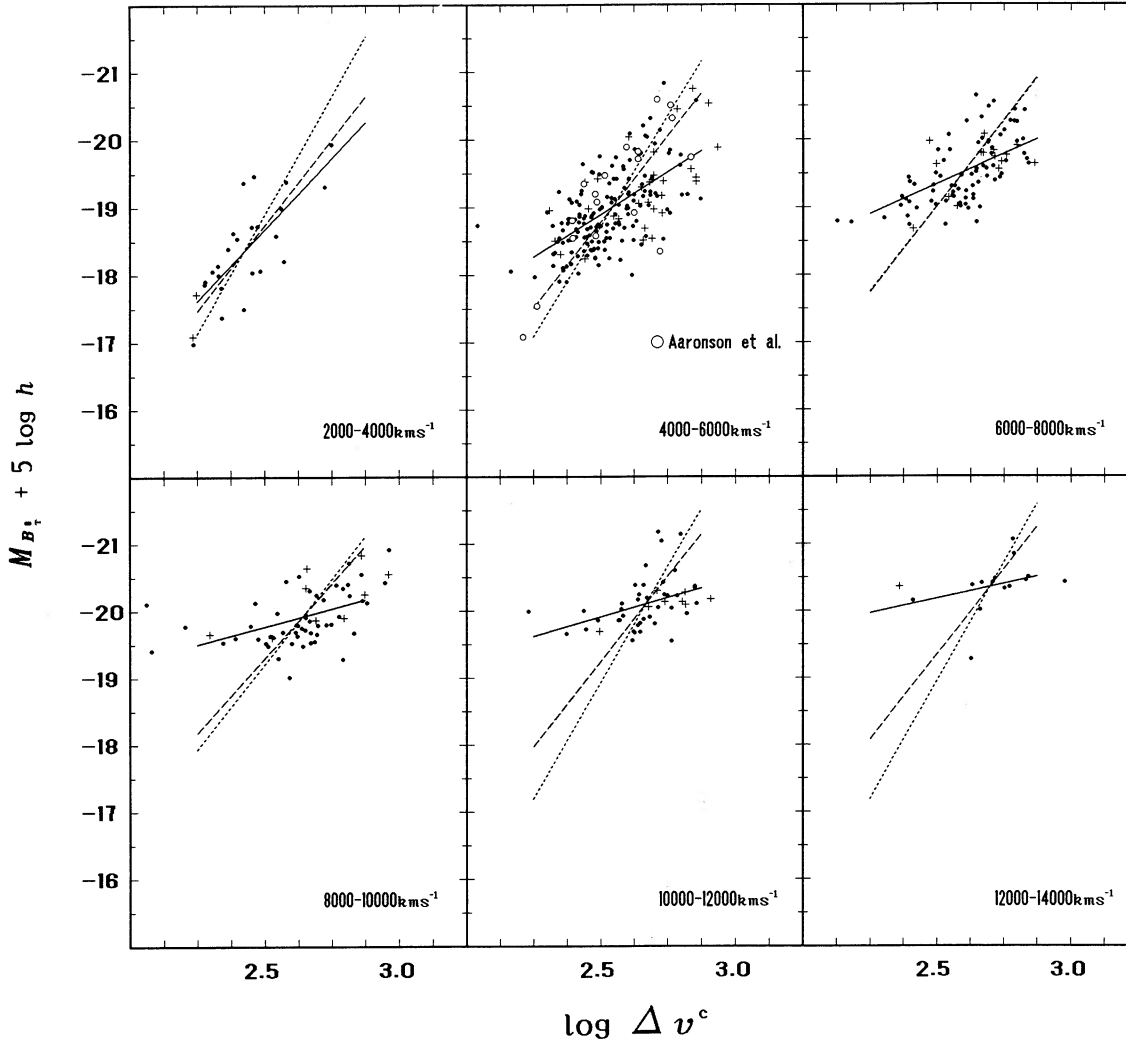


FIG. 11.—TF relations for the galaxies in recession velocity bins of 2000 km s^{-1} in the Pisces-Perseus region. Solid lines show the result of a two-parameter least-squares fit (fit [i]), and dashed lines show one-parameter fits with the slope parameter fixed at $B = 6.35$ (fit [ii]), the value for the local calibrator. Fitting using Schechter's prescription is depicted by dotted lines (fit [iii]). Absolute magnitudes are plotted with a default value of $h = 1$ ($h = H_0/100 \text{ km s}^{-1} \text{ Mpc}^{-1}$). To show the morphological dependence Sa and Sab galaxies are marked by plus signs. The galaxies in the sample used by Aaronson et al. (1986) are indicated by open circles in the panel corresponding to the $V_c = 4000\text{--}6000 \text{ km s}^{-1}$ velocity bin.

measurement is not biased. In fact, we obtained a slope parameter in fit (iii), which apparently remains constant independent of the distance of the sample, demonstrating that the proposed method indeed works. Errors of the slope parameter, however, rapidly increase as the distance increases, which makes it difficult to extract reliable parameters of the TF relation from the fit. This is because the fit is made with galaxies, whose magnitudes are distributed over a very limited magnitude range, e.g., less than 1 mag for the sample with the distance of $\sim 10,000 \text{ km s}^{-1}$. The dispersion of the fit also amounts to 1–1.6 mag, much larger than that for fit (i).

3.3 Morphological Dependence

Some doubt has often been cast on the universality of the TF relations (Robert 1978; Rubin et al. 1985; Giraud 1986; KCT). In particular, some morphological type of dependence has been proposed by several authors for the blue-band TF relations. We examine the morphological-type dependence in

Figure 11, where the data points for Sa–Sab are marked by different symbols. We do not observe particularly different behavior with early-type spirals in samples of any velocity bins. We also do not observe any type dependence for other spiral types in the range Sa–S/Irr. If the absorption correction of the RSA scheme is adopted instead, however, a morphological dependence appears. Rubin et al. (1985) and KCT suggested a strong morphological-type dependence; earlier type galaxies are fainter at a given line width than later types. They also suggested that there is no evidence that Sa galaxies follow the TF relation. We found that the large absorption correction for Sa–Sab galaxies in the RSA scheme is largely, if not entirely, responsible for their claim. Fouqué et al. (1990) and Kodaira & Watanabe (1988) also claimed that the internal absorption corrections of the RSA scheme, which gives total internal absorption magnitudes for Sa–Sb types 3 times as large as those of Sdm–Im galaxies, lead to overestimates for early types and underestimates for late types.

TABLE 4
PARAMETERS OF THE TF RELATION IN THE P-P REGION

V_c (1)	n (2)	Fit (i)			Fit (ii)			Fit (iii)		
		A (3)	B (4)	σ (5)	A (6)	σ (7)	h (8)	A (9)	B (10)	σ (11)
2000–4000	26	18.67 ± 0.11	5.29 ± 0.89	0.49	18.74 ± 0.75	0.49	0.84	18.89 ± 0.36	8.80 ± 1.46	1.59
4000–6000	204	18.90 ± 0.03	3.15 ± 0.28	0.48	18.78 ± 0.09	0.61	0.86	18.71 ± 0.09	8.14 ± 0.72	1.31
6000–8000	95	19.34 ± 0.05	2.20 ± 0.31	0.38	19.00 ± 0.20	0.65	0.95	19.01 ± 0.16	6.27 ± 0.89	1.55
8000–10000	61	19.78 ± 0.06	1.35 ± 0.31	0.36	19.20 ± 0.32	0.84	1.04	19.29 ± 0.17	5.58 ± 1.29	1.35
10000–12000	48	19.91 ± 0.08	1.41 ± 0.47	0.34	19.24 ± 0.41	0.63	1.06	18.92 ± 0.17	8.64 ± 2.88	1.18
12000–14000	15	20.19 ± 0.16	1.09 ± 0.80	0.38	19.34 ± 1.38	0.76	1.11	18.94 ± 0.24	8.79 ± 6.49	0.93

NOTE.—Fit (i) is the standard Tully-Fisher fit with two free parameters. Fit (ii) is similar to fit (i), but the slope parameter is fixed on the local value ($B = 6.35$). Fit (iii) uses Schechter's prescription.

4. MALMQUIST BIAS

4.1. Hubble Ratios

Hubble ratios V_c/r are shown in Figure 12 as a function of the H I line width $p = \log \Delta v^c$ for galaxies in each velocity bin. Here the recession velocity V_c is the value with respect to the CMB rest frame and r is the distance obtained from the TF relation with the aid of calibration (10). We adopt the RC2 absorption corrections. The obvious feature in this figure is that Hubble ratios increase toward a smaller p . This is the manifestation of the Malmquist bias. The trend is apparently more conspicuous for distant galaxy samples. The scatter of the data points corresponds to a dispersion of $\sigma = 0.4$ – 0.5 mag.

Figure 13 shows the Hubble ratios of the galaxies with a specified H I line width as a function of the recession velocity. This figure shows that the galaxies with line width $p = 2.3$ – 2.4 receive a significant bias even at distances as close as 2000–4000 km s⁻¹. The effect becomes smaller as p increases. For example, galaxies in the supercluster region ($V_c = 4000$ – 6000 km s⁻¹) suffer little from the bias, if $p \geq 2.6$. Hence, the average of the Hubble ratio for 46 galaxies with $2.6 \leq p \leq 2.7$, $\langle V_c/r \rangle = 75.8 \pm 3.1$ km s⁻¹ (the error is statistical only) should already be close to the true value of the Hubble constant from this supercluster.

4.2. Correction for the Malmquist Bias

Let $N(M, p)dM dp$ be the number density of galaxies in the interval (M to $M + dM$, p to $p + dp$). Then the average absolute magnitude of the observed sample located at distance $r_1 < r < r_2$ for a given H I line width p is brighter than the true average of absolute magnitudes by

$$\Delta M_p = \frac{\int_{r_1}^{r_2} dr r^2 \int_{-\infty}^{M_L(r)} dM M f(m_0) N(M, p)}{\int_{r_1}^{r_2} dr r^2 \int_{-\infty}^{M_L(r)} dM f(m_0) N(M, p)} - \frac{\int_{-\infty}^{+\infty} dM M N(M, p)}{\int_{-\infty}^{+\infty} dM N(M, p)}, \quad (13)$$

where $M_L(r) = m_{0L} - 5 \log (r/10 \text{ pc})$, with m_{0L} the limiting magnitude, and $f(m_0)$ is the selection function in corrected magnitudes as given in equation (9). Following Teerikorpi

(1984, 1987), we assume

$$N(M, p) = \phi(M)(2\pi)^{1/2} \sigma_p \exp \left\{ -[p - p(M)]^2 / 2\sigma_p^2 \right\}. \quad (14)$$

We also assume the universal luminosity function $\phi(M)$ used in equation (8). The dispersion σ_p is set equal to $\sigma_p = \sigma/B$ with B the slope of the local calibrator and σ the effective dispersion of the TF relation. The bias ΔM_p is directly interpreted as that in the distance scale.

It is not important to retain the r -dependence of ϕ^* , because we work with galaxies in distance bins and the r -dependence of ϕ^* largely cancels out over the numerator and the denominator in equation (13). We have checked this point by retaining the r -dependence of ϕ^* and using the density distribution given in Figure 10. We have found that the effect of inhomogeneity of the density distribution on ΔM_p is at most 0.04 mag for small p for the 4000–6000 km s⁻¹ region where the density changes sharply. For large p the effect is negligible.

The curves in Figures 12 and 13 show the prediction of the Hubble ratios using this formalism, as a function of $\log \Delta v^c$ for $H_0 = 75$ km s⁻¹ Mpc⁻¹ and $\sigma = 0.5$ mag with the dotted curves ± 0.5 mag (1 σ) from the predicted curves. To make a clear inspection of bias, we exemplify in Figure 14 the Hubble ratio for $p = 2.5$ – 2.6 (Figs. 14a and 14b) and for $p = 2.6$ – 2.7 (Figs. 14c and 14d). The data points in this figure represent the average $\langle V_c/r \rangle$ over galaxies with specified recession velocities, and their errors are calculated as dispersion divided by the square root of the number of galaxies. The curves in Figures 14a and 14c are obtained by varying σ from 0.3 to 0.8 with H_0 fixed at 75 km s⁻¹ Mpc⁻¹. In Figures 14b and 14d the case (H_0, σ) = (75, 0.5) is compared with the prediction with (H_0, σ) = (100, 0.3) and (50, 0.8). (The dashed curve added in Fig. 14a is for the case of $\sigma = 0.5$ with the density distribution of Fig. 10 explicitly taken into account in ϕ^* in order to demonstrate that the inhomogeneity effect is indeed small.) The increase of $\langle V_c/r \rangle$ with distance is indeed accounted for by the Malmquist bias, and the curve with (75, 0.5) gives an excellent fit over the distance range from 3000 to 11,000 km s⁻¹. Figures 14b and 14d demonstrate clearly that the cases with (H_0, σ) = (100, 0.3) and (50, 0.8) are excluded. The fact that the data points in Figure 15 are fitted well with a simple curve implies that large-scale peculiar velocities are considerably

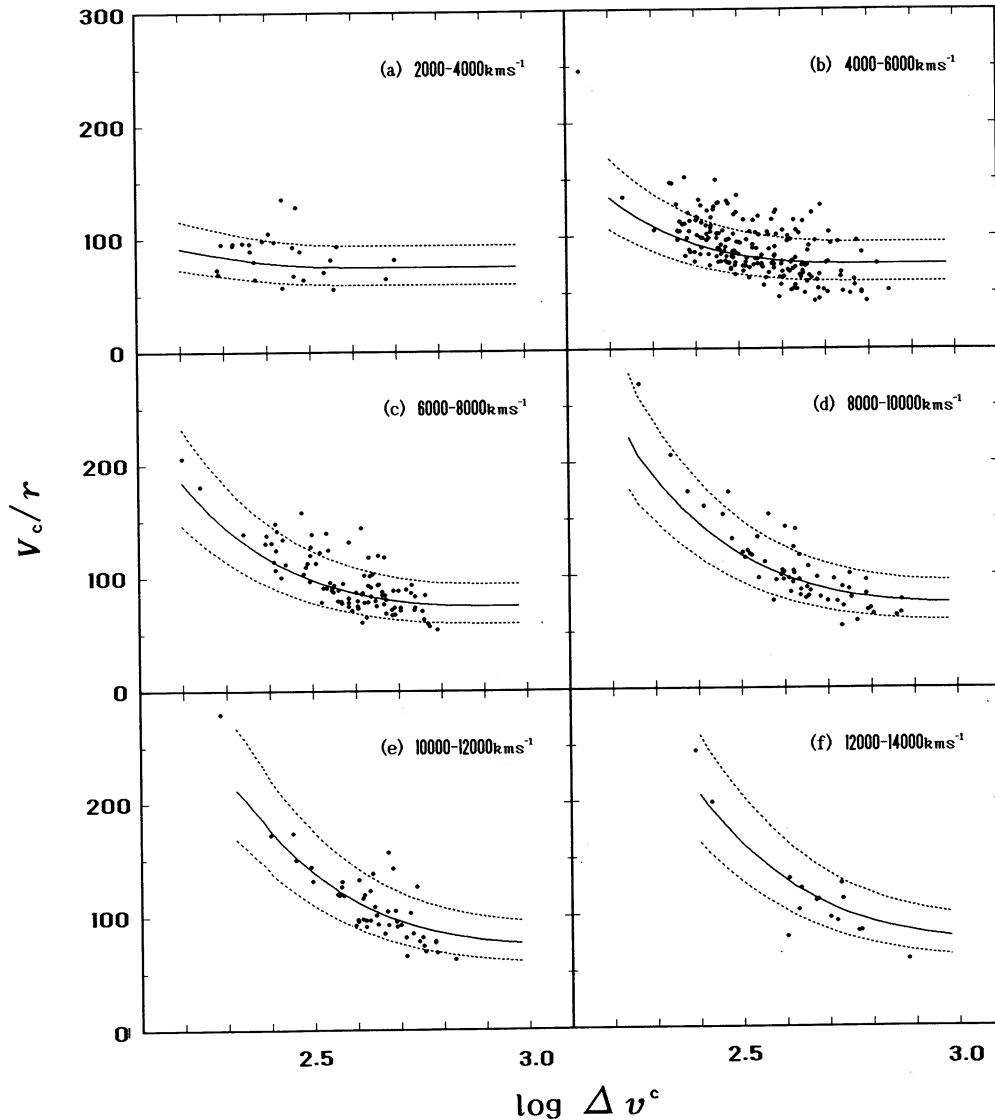


FIG. 12.—Hubble ratios derived with the use of the TF relation for galaxies in each recession velocity bin as a function of the logarithm of corrected H I line widths. Solid curves show the prediction of the model discussed in the text corresponding to $H_0 = 75 \text{ km s}^{-1} \text{ Mpc}^{-1}$ and the dispersion $\sigma = 0.5 \text{ mag}$. Dotted lines show the 1σ range.

smaller than the Hubble velocity over the region from 2000 to 12,000 km s^{-1} .

A similar analysis is made with Figure 12, which shows the effect of the Malmquist bias as a function of the H I line widths for galaxies with fixed recession velocity (Fig. 15). The curves presented in this figure are obtained in the same way as those for Figure 14. We show the data for the bins $V_c = 4000\text{--}6000 \text{ km s}^{-1}$ and $V_c = 6000\text{--}8000 \text{ km s}^{-1}$, where more galaxies are available. The data points are the average over galaxies shown in Figure 12 grouped into the $\Delta p = 0.05 \text{ H I}$ line width, and the curves are written with the same parameter sets as for Figure 14. While a reasonable agreement is seen between the data and the curve with $(75, 0.5)$, the curve slightly underestimates the bias for small H I line widths. In fact, a larger σ , $\sigma = 0.6 \text{ mag}$ say, brings the curve into a good agreement with the data. Such a dispersion, however, is somewhat larger than is actually found with the scatter of data points around the curve. We also

remark that the data points for the largest $\log \Delta v^c$ bin ($\log \Delta v^c = 2.75\text{--}2.8$) do not fall on the curve.⁴

To summarize our analysis, we show in Table 5 the Hubble constant derived from the galaxies in each bin for the case with $\sigma = 0.45 \text{ mag}$, together with the value obtained by simply averaging the Hubble ratio for each galaxy. The parameters are obtained for galaxies with $2.35 < \log \Delta v^c < 2.75$. We found that the derived Hubble constant stays constant within error as the distance increases for the choice of $\sigma = 0.4 \pm 0.05 \text{ mag}$. The dispersions σ_{H_0} listed in Table 5 correspond to $\sigma \simeq 0.40\text{--}0.55$

⁴ The data in the largest H I velocity width bin always deviate from the curve expected from the data for $\log \Delta v^c < 2.75$. This might be ascribed to some nonlinearity of the TF relation at the most luminous side. Without knowing the reason, we omit these data from the fit in our analysis. We also note that they are outside the range of the line width for which local calibration is available.

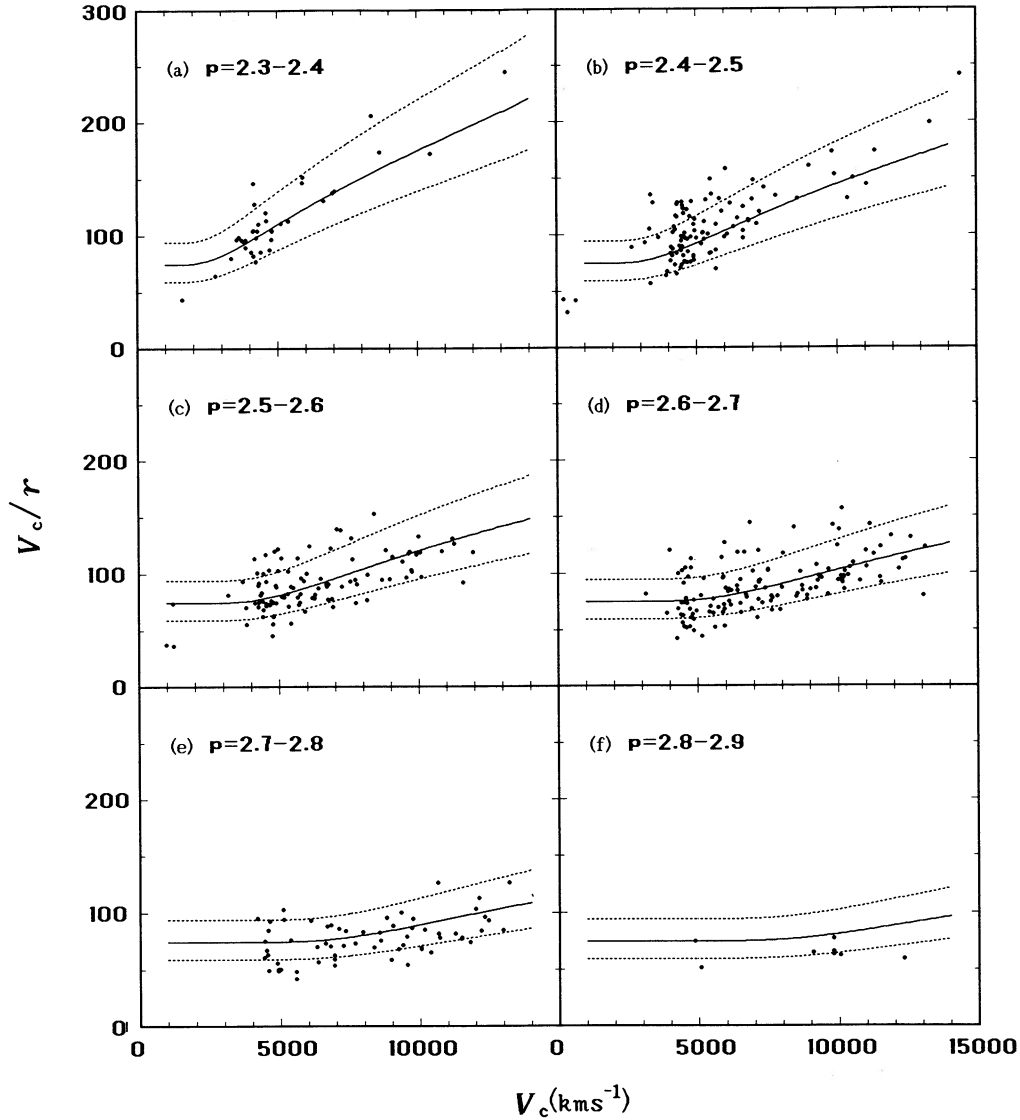


FIG. 13.—Hubble ratios for galaxies with a specified line width as a function of distance (recession velocity V_c). Solid curves show the prediction of the model for $H_0 = 75 \text{ km s}^{-1} \text{ Mpc}^{-1}$ and $\sigma = 0.5 \text{ mag}$. Dotted lines indicate the 1σ range.

mag. With $\sigma = 0.45$ we conclude from the sample in the range $2000 \text{ km s}^{-1} < V_c < 14,000 \text{ km s}^{-1}$ (392 galaxies) that

$$H_0 = 78.5 \pm 0.9 \text{ km s}^{-1} \text{ Mpc}^{-1} \quad (15)$$

TABLE 5
HUBBLE RATIOS FOR VELOCITY BINS

V_c	n	Nominal Average	H_0 ($\sigma_{TF} = 0.45$)	σ_{H_0}	Mean Error
2000–4000	20	85.6	81.8	21.4	4.8
4000–6000	189	88.6	79.9	18.6	1.4
6000–8000	85	96.3	79.0	17.1	1.9
8000–10000	46	106.2	74.6	18.8	2.8
10000–12000	40	112.5	73.2	17.5	2.8
12000–14000	12	127.8	74.0	22.9	6.6
2000–14000	392	95.8	78.5	18.4	0.9

NOTE.—Fits for galaxies of $\log \Delta v^i = 2.35\text{--}2.75$. Mean errors are calculated as $\sigma_{H_0}/n^{1/2}$.

with respect to the CMB rest frame. Here the error is statistical only. We also conclude that the Hubble flow in the Pisces-Perseus supercluster region is almost uniform, allowing, however, a variation by up to $\pm 5\%$ in the effective H_0 in the distance range $2000\text{--}15,000 \text{ km s}^{-1}$. Though unlikely, a slight decrease of H_0 with distance is not excluded from the data. If we take the Local Group centroid, instead of the CMB rest frame, a similar analysis yields

$$H_0 = 83.2 \pm 1.0 \text{ km s}^{-1} \text{ Mpc}^{-1} \quad (16)$$

A table similar to Table 5, but for p bins, is also presented for $\sigma = 0.45 \text{ mag}$ (Table 6). We observe that H_0 depends on p only weakly.

In order to confirm that the value (15) represents an unbiased estimate for the Hubble constant, we attempt to combine all data presented in Figure 13 by plotting the Hubble ratio as a function of the distance (recession velocity) defined

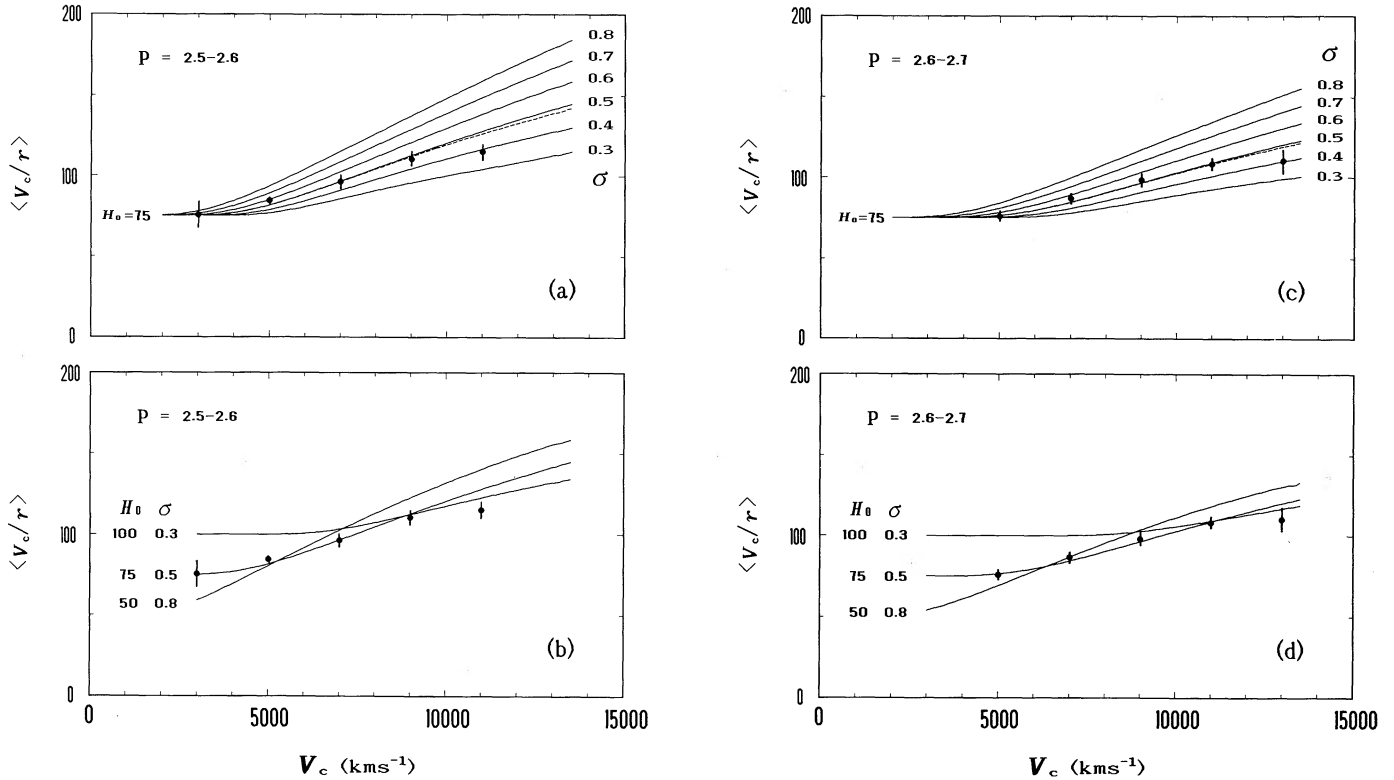


FIG. 14.—(a) Hubble ratios as a function of distance (recession velocity V_c) for galaxies with the H I line width $2.5 \leq p = \log \Delta v^c < 2.6$, compared with model predictions. The data points are obtained by averaging those of Fig. 13 over galaxies in the respective recession velocity bins, and attached bars are mean errors (dispersion divided by the square root of the number of galaxies). The curves correspond to the model with the Hubble constant fixed at $H_0 = 75 \text{ km s}^{-1} \text{ Mpc}^{-1}$ with various values of the dispersion. The dashed curve shows the prediction for an inhomogeneous galaxy distribution for the case of $\sigma = 0.5 \text{ mag}$. (b) Same as (a), but compared with the Malmquist bias models: $H_0 = 75 \text{ km s}^{-1} \text{ Mpc}^{-1}$, $\sigma = 0.5 \text{ mag}$; $H_0 = 100 \text{ km s}^{-1} \text{ Mpc}^{-1}$, $\sigma = 0.3 \text{ mag}$; and $H_0 = 50 \text{ km s}^{-1} \text{ Mpc}^{-1}$, $\sigma = 0.8 \text{ mag}$. (c) Same as (a), but for $2.6 \leq p < 2.7$. (d) Same as (b), but for $2.6 \leq p < 2.7$.

by

$$V_c^* = V_c \times 10^{-0.2B(\log \Delta v^c - 2.5)} \quad (17)$$

(Bottinelli et al. 1986), assuming that the Hubble flow is uniform. Here we normalized $V_c^* = V_c$ at $\log \Delta v^c = 2.5$. With this distance the Malmquist bias enters in the same way irrespective of the intrinsic luminosity of galaxies. We show in Figure 16 the $V_c/r - V_c^*$ diagram. We see that our model curve with $H_0 = 75 \text{ km s}^{-1} \text{ Mpc}^{-1}$, $\sigma = 0.5 \text{ mag}$ falls in the middle of the data points. With this prescription we can increase the number of data points in the plateau region; with 109 galaxies in the range $2000 \text{ km s}^{-1} \leq V_c^* \leq 4000 \text{ km s}^{-1}$ we find $\langle V_c/r \rangle = 76.1 \pm 1.9 \text{ km s}^{-1} \text{ Mpc}^{-1}$, which is in good agreement with equation (15). In a similar way we combine the data

in Figure 12 using the variable

$$\log \Delta v^* = \log \Delta v^c - \frac{1}{0.2B} \log \left(\frac{V_c}{5000 \text{ km s}^{-1}} \right), \quad (18)$$

with the normalization taken at $V_c = 5000 \text{ km s}^{-1}$ (see Fig. 17). From 82 galaxies in the plateau region, $\log \Delta v^* = 2.6\text{--}2.75$, we may also find a consistent value $\langle V_c/r \rangle = 75.7 \pm 2.0 \text{ km s}^{-1} \text{ Mpc}^{-1}$.

4.3. Analysis with a Reduced-Size Sample

For a further check of the consistency of our formalism, we repeated our analysis with a magnitude-limited sample of $B_T^0 \leq 14.5$. We show galaxies with $B_T^0 \leq 14.5 \text{ mag}$ and the prediction from equation (13) with the selection function set equal to $f(m_0) = 1$ for $m_0 \leq 14.5$ and $f(m_0) = 0$ for $m_0 > 14.5$; the case $H_0 = 75 \text{ km s}^{-1} \text{ Mpc}^{-1}$, $\sigma = 0.5 \text{ mag}$ is shown in Figure 18 for $V_c = 4000\text{--}6000 \text{ km s}^{-1}$ and in Figure 19 for $\log \Delta v^c = 2.6\text{--}2.7$. While the sample suffers a significantly stronger bias than that seen in Figure 12 and in Figure 13 in low velocity width or in distant bins, our model successfully traces the observations. In fact, H_0 from Figure 18 ($H_0 = 76.7$, with mean error $\pm 1.7 \text{ km s}^{-1} \text{ Mpc}^{-1}$) agrees with $H_0 = 79.9 \pm 1.4 \text{ km s}^{-1} \text{ Mpc}^{-1}$ derived from the original data set for the same V_c bin. From Figure 18 we obtain $H_0 = 73.8 \text{ km s}^{-1} \text{ Mpc}^{-1}$, with mean error $\pm 1.8 \text{ km s}^{-1} \text{ Mpc}^{-1}$, which is compared with the value from the full sample $H_0 = 75.5 \pm 1.7 \text{ km s}^{-1} \text{ Mpc}^{-1}$. This confirms that the estimated Hubble constant depends little on the Malmquist bias, once it is controlled

TABLE 6

HUBBLE RATIOS FOR VELOCITY WIDTH BINS

p	n	Nominal Average	H_0 ($\sigma_{\text{TF}} = 0.45$)	σ_{H_0}	Mean Error
2.3–2.4	36	116.3	82.7	16.4	2.7
2.4–2.5	101	108.2	85.2	18.8	1.9
2.5–2.6	99	92.9	76.1	17.6	1.8
2.6–2.7	131	89.1	75.5	19.1	1.7
2.7–2.8	63	77.8	69.7	15.7	2.0

NOTE.—Fits for galaxies in $V_c = 2000\text{--}15,000 \text{ km s}^{-1}$. Mean errors are calculated as $\sigma_{H_0}/n^{1/2}$.

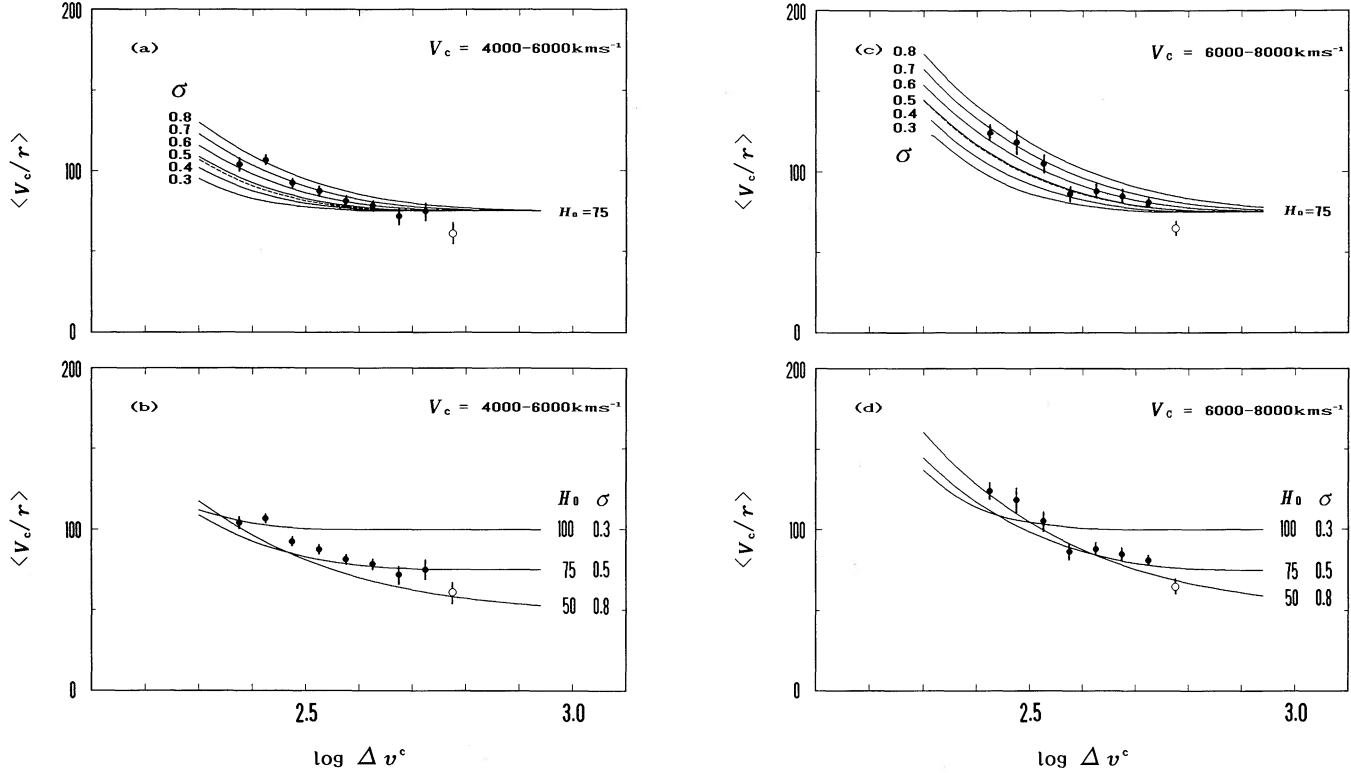


FIG. 15.—(a) Hubble ratios as a function of the H I line width for galaxies located in the $V_c = 4000\text{--}6000 \text{ km s}^{-1}$ region, as compared with the model prediction discussed in the text. The data points are obtained by averaging those of Fig. 12 over galaxies in the respective $\log \Delta v^c$ bins, and attached bars are mean errors (dispersion divided by the square root of the number of galaxies). The curves correspond to the model with the Hubble constant fixed at $H_0 = 75 \text{ km s}^{-1} \text{ Mpc}^{-1}$ with various values of the dispersion. The dashed curve shows the prediction with corrections for an inhomogeneous galaxy distribution for the case of $\sigma = 0.5 \text{ mag}$. (b) Same as (a), but compared with three typical models: $H_0 = 75 \text{ km s}^{-1} \text{ Mpc}^{-1}$, $\sigma = 0.5 \text{ mag}$; $H_0 = 100 \text{ km s}^{-1} \text{ Mpc}^{-1}$, $\sigma = 0.3 \text{ mag}$; and $H_0 = 50 \text{ km s}^{-1} \text{ Mpc}^{-1}$, $\sigma = 0.8 \text{ mag}$. (c) Same as (a), but for $V_c = 6000\text{--}8000 \text{ km s}^{-1}$. (d) Same as (b), but for $V_c = 6000\text{--}8000 \text{ km s}^{-1}$.

properly. In Figure 18 the 18 galaxies in the sample of Aaronson et al. (1986) are depicted by open circles. (Two data points located at the left are galaxies which do not satisfy $m_Z \leq 15.7 \text{ mag}$ and hence were removed from our analysis.) This shows that the Aaronson et al. sample is almost a random subset of the $B_T^0 \leq 14.5 \text{ mag}$ complete sample.

5. DISCUSSION

5.1. The Hubble Constant

We have obtained the global value of the Hubble constant in equation (15) from 393 Arecibo galaxies in the range $V_c = 2000\text{--}15,000 \text{ km s}^{-1}$ with $\log \Delta v^c = 2.35\text{--}2.75$, selecting Sa-Sc/

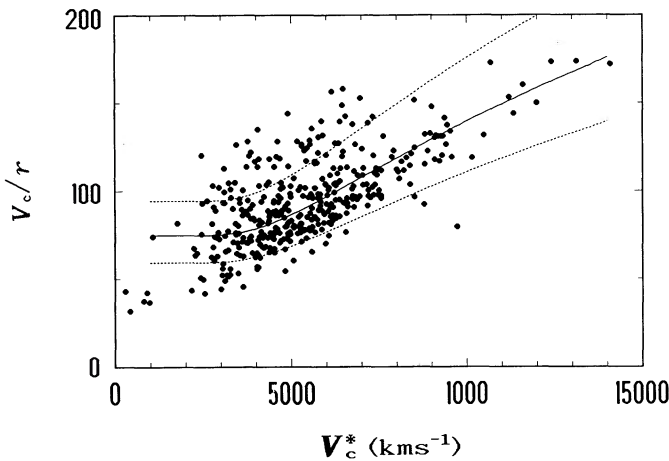


FIG. 16.—Hubble ratios V_c/r as a function of V_c^* defined in eq. (17). The solid curve shows the prediction of the model for $H_0 = 75 \text{ km s}^{-1} \text{ Mpc}^{-1}$ and $\sigma = 0.5 \text{ mag}$. Dotted lines indicate the 1σ range.

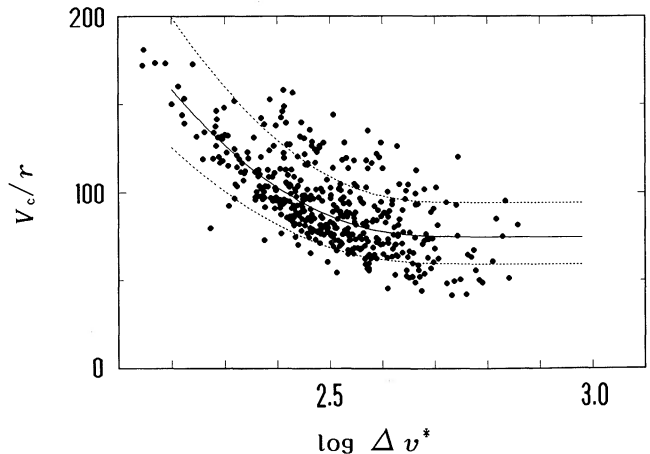


FIG. 17.—Hubble ratios V_c/r as a function of $\log \Delta v^*$ defined in eq. (18). The meaning of the curves is the same as Fig. 16.

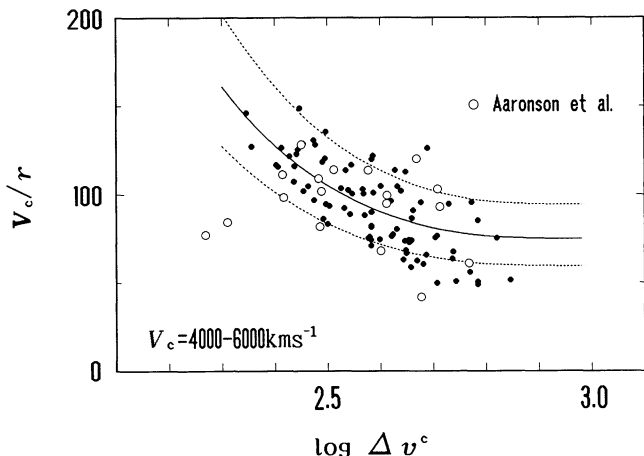


FIG. 18.—Hubble ratios as a function of the H I line width for the magnitude-limited sample of $B_T^0 \leq 14.5$ mag in $V_c = 4000\text{--}6000$ km s $^{-1}$ (P-P supercluster region). Open circles show the sample of Aaronson et al. (1986) (the two farthest left points are not included in the Arecibo sample). The curves correspond to the model $H_0 = 75$ km s $^{-1}$ Mpc $^{-1}$, $\sigma = 0.5$ mag, with 1σ dispersion denoted by dotted curve.

Irr morphological types and $i \geq 45^\circ$ with respect to the CMB rest frame, or the value in equation (16) with respect to the Local Group centroid, after the correction for the Malmquist bias. If a simple mean of the Hubble ratios was taken over the full sample, we are led to, e.g., $H_0 = 96.2$ km s $^{-1}$ Mpc $^{-1}$ in the CMB rest frame. The correction depends on the dispersion of the TF plot, but little on the precise parameters of the luminosity function or on inhomogeneous distributions of galaxies. We found that a satisfactory description is obtained with $\sigma = 0.4\text{--}0.5$ mag of the TF relation.

In Figure 13 we see that six galaxies with $V_c < 2000$ km s $^{-1}$ (one point in Fig. 13a, three points in Fig. 13b, and two points in Fig. 13c) deviate from the predicted curve. This could be ascribed to a peculiar velocity flow near the Local Supercluster. We do not see any indication that the supercluster in the velocity range $V_c = 4000\text{--}6000$ km s $^{-1}$ is moving relative

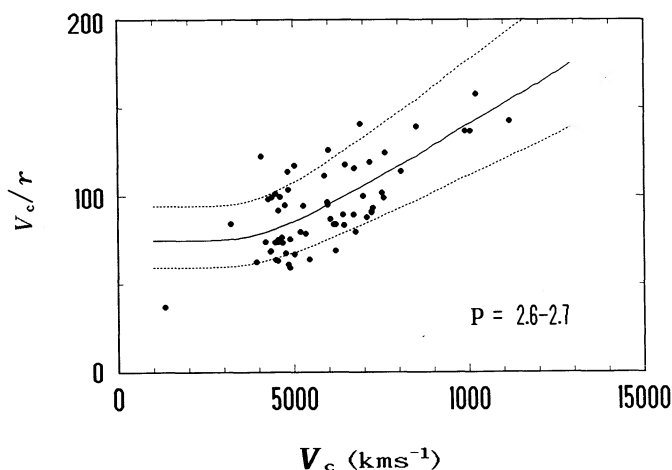


FIG. 19.—Hubble ratios as a function of the recession velocity for the magnitude-limited sample of $B_T^0 \leq 14.5$ mag for $p = 2.6\text{--}2.7$. The curves correspond to the model $H_0 = 75$ km s $^{-1}$ Mpc $^{-1}$, $\sigma = 0.5$ mag, with 1σ dispersion denoted by dotted curve.

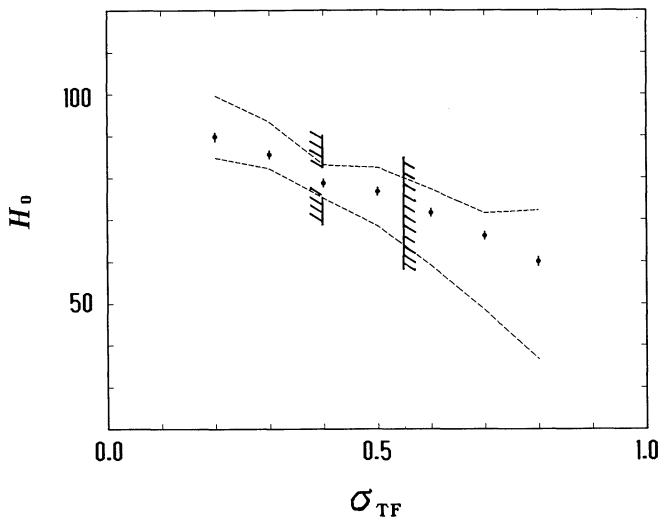


FIG. 20.—Hubble constant corrected for the Malmquist bias as a function of the dispersion σ_{TF} of the TF relation. The dashed curves indicate the maximum and minimum values of the Hubble constant obtained for each velocity bin or H I line-width bin, as in Tables 5 and 6. The region between the two hatched boundaries shows the range of σ_{TF} , with which we obtain a reasonable fit to the data.

to foreground or background galaxies. Furthermore, we do not observe any larger peculiar velocities inside the supercluster. The brightest class of galaxies ($\log \Delta v^c > 2.75$) shows some deviation from the behavior expected from fainter galaxies; the Hubble ratios for these galaxies (69.6 km s $^{-1}$ Mpc $^{-1}$ in average, $\sigma = 14.2$) are systematically smaller than for others. This might indicate some departure (downward) of the 21 cm line width–luminosity relation from linearity. We note that a similar trend is seen for $\log \Delta v^c > 2.75$ in the TF plot for the Virgo and UMa galaxies given by Tully (1988). No departure from a linear relationship is observed for $\log \Delta v^c < 2.75$. Non-linearity is also not detected in the local calibrators ($\log \Delta v^c < 2.75$, however) (Fukugita et al. 1991).

5.2. Estimates of Uncertainties of the Hubble Constant

Uncertainties are divided into random errors and systematic biases. An extensive study for the sources of errors was made by Fukugita et al. (1991). Based on their discussion, we examine errors for the present Hubble constant. Random errors are estimated by dividing a quadrature sum of the dispersions by a square root of the number of galaxies, and systematic errors by adding quadratures. The large size of the present sample makes random errors generally quite small. The most important among them is the error arising from the net dispersion of the TF relation ($0.4\text{--}0.5$ mag). Dividing this value by the square root of the number of galaxies, we obtain $0.020\text{--}0.025$ mag, which corresponds to $\sim 1\%$ in H_0 .

Uncertainties in the absorption correction largely tend to cancel out between the Arecibo sample and the local calibrators, as seen in Table 3 and discussed in detail in § 2.6. The net uncertainty in $A_B + A_i$ arising from the choice of correction scheme is less than 0.14 mag. In fact, the Hubble constant derived from the TF relation using the absorption corrections of the RSA scheme is 79.4 km s $^{-1}$ Mpc $^{-1}$, which differs from the value derived by the RC2 scheme only by 1% (0.02 mag).

As we discussed in § 2.2, there may be a zero-point error of photometry in the calibrating galaxies of LdV; if we adopt the

zero point set by the photometry of Bothun et al. (1985), our P-P galaxies become 0.09 mag fainter. We may also expect $\lesssim 0.1$ mag error in the zero point of the corrected Zwicky magnitude. The random error of the corrected Zwicky magnitude contributes only to increasing the dispersion of the TF relation.⁵

We have also examined the effect of the inclination cut. A relaxation of the cut to $i > 35^\circ$ increases the number of galaxies to 428, which results in $H_0 = 78.9 \text{ km s}^{-1} \text{ Mpc}^{-1}$. If we further restrict the inclination between 45° and 75° to avoid edge-on spirals, for which internal absorption might cause an error in the galaxy brightness, we are led to $H_0 = 80.8 \text{ km s}^{-1} \text{ Mpc}^{-1}$ from 284 galaxies. Hence the error is of the order of 3%.

The estimate of the net dispersion of the TF relation is uncertain by ± 0.1 mag, which results in an error for the Hubble constant through the correction for the Malmquist bias. In Figure 20 we plot the dependence of the corrected Hubble constant upon the dispersion of the TF relation. From this figure it is estimated that $\Delta\sigma_{\text{TF}} = \pm 0.1$ mag causes an uncertainty of $\mp 6\%$ in H_0 (± 0.13 mag in distance). We also studied the uncertainty arising from that of the slope parameter for the local calibrators. We find that $\Delta B = \pm 1$ leads to $|\Delta H_0| = 1.5 \text{ km s}^{-1} \text{ Mpc}^{-1}$.

The TF relation for local calibrators (fit I of Fukugita et al. 1991) has an intrinsic scatter of 0.4 mag, which brings a random error of 0.14 mag. The zero point of the local calibrators is uncertain perhaps by ± 0.15 mag in view of recently

⁵ We also made an analysis taking into account the fact that the random error of the Zwicky magnitude increases as galaxies become fainter. The results are virtually the same as those presented in this paper.

discussed uncertainty (Feast 1991). If we accept a consistent data set for five galaxies by Freedman (1990), the dispersion of the TF relation is reduced to 0.25 mag with a zero point 0.08 mag brighter (Fukugita et al. 1991). With this calibration H_0 becomes $75.8 \text{ km s}^{-1} \text{ Mpc}^{-1}$. Finally, the method of velocity correction for the recession velocity may also be counted as a source of uncertainty in H_0 : the value of the Hubble constant using V_{LG} ($H_0 = 83.2 \text{ km s}^{-1} \text{ Mpc}^{-1}$) decreases to $81.1 \text{ km s}^{-1} \text{ Mpc}^{-1}$ if the velocities are corrected for the 250 km s^{-1} Virgo infall motion of the Local Group. This corresponds to assuming that all galaxies in the P-P region are participating in bulk flow toward the apex of the cosmic microwave background anisotropy. A correction for the random motion corresponding to the local anomaly (Han & Mould 1990), when added to the Virgo infall, yields $H_0 = 81.5 \text{ km s}^{-1} \text{ Mpc}^{-1}$.

From our analysis we conclude that $H_0 = 78.5 \pm 5.5_{-7.2}^{+8.7} \text{ km s}^{-1} \text{ Mpc}^{-1}$ for the CMB rest frame and $H_0 = 83.2 \pm 5.8_{-7.6}^{+9.2} \text{ km s}^{-1} \text{ Mpc}^{-1}$ with respect to the Local Group centroid, where the first error is of random nature and the second is systematic errors, both obtained by quadrature separately. The errors discussed here are summarized in Table 7.

5.3. Intrinsic Dispersion of the TF Relation

The net dispersion of the TF relation, $\sigma \approx 0.45\text{--}0.5$ mag, includes the scatter arising from errors of observations and those from corrections made to individual galaxies as well as the intrinsic scatter. The random peculiar velocity of galaxies also contributes to the dispersion. Therefore, it may be difficult to estimate the intrinsic dispersion of the TF relation. The corrected Zwicky magnitude error should contribute by

TABLE 7
UNCERTAINTIES FOR THE HUBBLE CONSTANT

SOURCE OF ERRORS	DISPERSION (mag)	ERRORS IN H_0 (%)	
		Random	Bias
P-P Region ($n = 393$)			
H I line-width data (including transformation to ΔV_{20})	0.15	0.4	...
Inclination correction:			
Errors in b/a	0.08	0.2	...
Formula model dependence (0.05 mag)	± 2.3
Photometry:			
Zero point (0.1 mag)	± 4.7
Random error of m_z	0.26	0.6	...
Absorption corrections $A_B + A_i$	$+14.3^*$
K-correction error	0.01	0.02	...
Scatter of the TF relation	0.45	1.0	...
Sample selection inclination cut	$+2.9$
Malmquist bias corrections:			
Selection functions	$+2.5$
Luminosity functions	-0.6
Dispersion of the TF relation	± 1.0
Local calibrator slope ($ \Delta B = 1$)	± 6.0
Local calibrator slope ($ \Delta B = 1$)	± 1.9
Local Calibrators ($n = 8$) (Fukugita et al. 1991)			
Local calibrator distance	-3.7
H I line width	0.098	1.6	...
Photometry	0.04	0.6	...
Absorption corrections (0.15 mag)	-7.9^*
TF relation scatter	0.40	6.7	...
Total uncertainty	...	± 7.0	$+11.1$ -9.1

NOTE.—Numbers with asterisks cancel between the P-P galaxies and the local calibrators.

$\sigma \approx 0.25$ mag. We would guess that the dispersion caused by the error in Galactic extinction is ≈ 0.09 mag (dispersion of the regression between RC2 and BH corrections). We also expect even larger scatter in the internal absorption correction. Errors in b/a ($\sigma \approx 10\%$) cause errors of line-width corrections and of internal absorption corrections, which amount to 0.08 and 0.03 mag, respectively, are of the same sign, and contribute to the dispersion of the TF relation. The error in H I line-width measurements and in the conversion of W_1 to ΔV_{20} gives $\sigma \approx 0.19$ mag. If the random peculiar velocity is about 10% of the Hubble flow in the 4000–8000 km s⁻¹ region, it further contributes to the dispersion by 0.2 mag. Taking these effects into account, we may guess that the intrinsic dispersion of the TF relation is $\sigma \approx 0.2$ –0.35 mag.

5.4. Comparison with the Analysis by Aaronson et al. (1986)

The Pisces sample considered by Aaronson et al. (1986) consists of 20 galaxies, 18 of which are contained in the Arecibo sample in the 4000–6000 km s⁻¹ bin (NGC 538 and NGC 575 are outside of the Arecibo survey strip). By averaging the Hubble ratios $\langle V_{LG}/r \rangle$ over 20 galaxies derived from the *H*-band TF relation (without correction for the Local Group motion with respect to CMB), they obtained $\langle V_{LG}/r \rangle = 102.9$ km s⁻¹ Mpc⁻¹ with the dispersion $\sigma = 19.6$ km s⁻¹ Mpc⁻¹. (This value becomes $\langle V_{LG}/r \rangle = 104.4$ km s⁻¹ Mpc⁻¹ with dispersion 19.1 km s⁻¹ Mpc⁻¹ if we ignore the above two galaxies.) Using *B*-band photometry data for the 18 galaxies used in our analysis, we found $\langle V_{LG}/r \rangle = 106.4$ km s⁻¹ Mpc⁻¹ with $\sigma = 24.7$ km s⁻¹ Mpc⁻¹. (For the local calibrator we used the distance moduli of three galaxies [M31, M33, and NGC 2403] of Aaronson et al. 1986 in agreement with their prescriptions; if we use the local calibrations used in this paper, eq. [10], we have $\langle V_{LG}/r \rangle = 105.7$ km s⁻¹ Mpc⁻¹ with $\sigma = 24.6$ km s⁻¹ Mpc⁻¹.) Our *B*-band TF relation with the sample of Aaronson et al. yields essentially the same result as their *H*-band TF analysis.

Of 18 galaxies, 16 satisfy $B_T^0 \leq 14.5$ mag. As is apparent in Figure 18, the sample of Aaronson et al. is regarded as an almost uniform selection of the magnitude-limited ($B_T^0 \leq 14.5$ mag) sample. They claimed that the sampling is sufficiently deep and that the Malmquist bias can be ignored. We see, however, in Figure 18 that the $B_T^0 \leq 14.5$ sample in the Pisces region receives a significant Malmquist bias. Assuming that the Aaronson et al. sample is a uniformly selected $B_T^0 \leq 14.5$ sample, we obtain $H_0(\text{Local Group centroid}) \approx 80.6$ km s⁻¹ Mpc⁻¹ from our model (UGC 679 and UGC 1066 galaxies [$\log \Delta v < 2.3$ and $m_z > 15.7$ mag] are excluded from the calculation). That is, their sample suffers from the Malmquist bias by 0.6 mag. We may expect that a similar situation happens also in the *H*-band TF analysis. We suggest that the high value of the Hubble constant ($H_0 \approx 90$ km s⁻¹ Mpc⁻¹) found by Aaronson et al. (1986) for the Pisces Cluster is caused by neglecting the Malmquist bias.

5.5. Comment on the Analysis by Bottinelli et al. (1987) and by KCT

Bottinelli et al. (1987) took the *B*-band photometry data from Bothun et al. (1985) for 23 galaxies. Of these, 19 are in the sample that we used (three are located outside the strip, and one has a low inclination $i = 20^\circ$ and hence is excluded in our analysis). The average of these data, $\langle V_{LG}/r \rangle = 106$ km s⁻¹ Mpc⁻¹ and $\sigma = 27$ km s⁻¹ Mpc⁻¹, agrees with our value, despite their use of the 0.2 mag fainter photometry data of

Bothun et al. This is partly explained by their local calibrator, which is 0.37 mag fainter than ours.

KCT used the Aaronson et al. sample, but deduced a distance modulus to the Pisces Cluster very different (1 mag fainter) from that by Aaronson et al. with both *B*- and *H*-band TF relations. KCT's fainter modulus arises from their conjecture that the galaxies used by Aaronson et al. should have suffered from a very strong Malmquist bias and hence should be brighter than the true average magnitude by ~ 1 –1.4 mag. Our analysis using the complete sample of $B_T^0 \leq 14.5$ shows that the conjecture made by KCT is not supported as discussed in § 5.4 above. Both our theoretical curve and analysis with the full sample show that brighter part of the Aaronson et al. sample is subject to only a small bias. We found a significant Malmquist bias (~ 0.6 mag) when galaxies with smaller H I line width are included, but we found that it is not as strong as that proposed by KCT; the “ 2σ upper envelope prescription” proposed by KCT gives an incorrect Hubble constant, as pointed out by other authors (Gavazzi & Trinchieri 1989; Fukugita et al. 1991).

5.6. Peculiar Velocity Flow

Willick (1990) carried out CCD photometry in the *R* band for 320 spiral galaxies in the Arecibo sample and studied the peculiar velocity field in the P-P supercluster region. He showed that nearly all galaxies with $cz \leq 2000$ km s⁻¹ have negative peculiar velocities (velocity toward the Local Group) with an amplitude of ~ 1000 km s⁻¹. Most important, he showed that the P-P supercluster located at ~ 5000 km s⁻¹ has a streaming motion velocity of ~ -450 km s⁻¹ toward the Local Group, and the great majority of objects in the background of the supercluster also have large negative peculiar velocities out to a redshift of ~ 7000 km s⁻¹, whereas the galaxies with $cz > 8000$ km s⁻¹ are at rest. He ascribed this large-scale streaming motion to low-amplitude density fluctuations on scales larger than $100 h^{-1}$ Mpc.

Let us examine his conclusion using our result, especially Figures 13 and 14. For the negative peculiar velocity up to $cz \sim 2000$ km s⁻¹, Figure 13 lends strong support for its existence. The Hubble ratios for galaxies in this region deviate largely from the predicted curve, indicating a negative peculiar velocity flow of the order of 1000 km s⁻¹. For more distant galaxies, the nominally increasing average Hubble constant ratios (as seen in Fig. 15), $\langle V_{LG}/r \rangle = 99$ km s⁻¹ Mpc⁻¹ ($V_{LG} = 4000$ –6000 km s⁻¹), 103 km s⁻¹ Mpc⁻¹ ($V_{LG} = 6000$ –8000 km s⁻¹), 109 km s⁻¹ Mpc⁻¹ ($V_{LG} = 8000$ –10,000 km s⁻¹), and 123 km s⁻¹ Mpc⁻¹ ($V_{LG} > 10,000$ km s⁻¹), are consistent with Willick's observation; the difference between $\langle V_{LG}/r \rangle = 99$ km s⁻¹ Mpc⁻¹ for $V_{LG} = 4000$ –6000 km s⁻¹ and $\langle V_{LG}/r \rangle$ for a greater distance yields -500 to -1000 km s⁻¹. As we have discussed in § 4, however, the increase of the Hubble ratio as the distance is explained by the Malmquist bias.

5.7. Comparison with the Analysis of Fukugita et al. (1991) for the Coma Cluster

Another case in which the Malmquist bias is quantitatively estimated is the analysis by Fukugita et al. (1991) for the Coma Cluster. The model that they used is very similar to the one described in § 4. With the same scheme adopted here (the RC2 absorption corrections, local calibrators, and LdV zero point for photometry) they obtained the distance modulus to the Coma Cluster $34.34 \pm 0.20^{+0.21}_{-0.09}$, which corresponds to $H_0 = 94^{+13}_{-16}$ km s⁻¹ Mpc⁻¹ with respect to the Local Group cen-

troid or $H_0 = 97_{-16}^{+14}$ km s⁻¹ Mpc⁻¹ with respect to the CMB rest frame.

At first glance the above values of H_0 appear to overlap with the values obtained in the present analysis. If we look at the procedure more carefully, however, we see that the error for the relative values of H_0 is much smaller, because a large part of the random error arises from the uncertainty for the local calibrator which does not enter into the ratios. From Table 7 of Fukugita et al. and the error estimate in § 6.2, we obtain

$$\frac{H_0(\text{P-P})}{H_0(\text{Coma})} = 0.81 \pm 0.05_{-0.09}^{+0.11} \text{ (CMB rest frame)}. \quad (19)$$

This discrepancy corresponding to 0.46 mag is significant. [If the Local Group centroid is used as a reference frame, $H_0(\text{P-P})/H_0(\text{Coma}) = 0.89 \pm 0.05_{-0.10}^{+0.12}$.] The correction for the local velocity flow with respect to the CMB makes the deviation even larger, contrary to the conclusion obtained in Aaronson et al. Let us study possible origins of the discrepancy ($\Delta m = 0.46$ mag): (1) Zero-point error of relative photometry. Both sets of photometry are based on the Kiso Schmidt plates, and the zero points are derived from the photometry data in the LdV compilation. The total magnitudes that we obtained are in accurate agreement with those of RC2. In particular $\langle B_T(\text{P-P}) \rangle - \langle B_T(\text{Coma}) \rangle$ is only $\Delta m = 0.04$ mag brighter than that with the magnitudes of RC2. The result is not changed by adopting the zero point of Bothun et al. (1985) ($\Delta m = -0.02$ mag); the zero-point offset between LdV and Bothun et al. cancels between the P-P galaxies and the Coma galaxies (see Table 2), and the residual yields $\Delta m = -0.04$ mag for B_T . We expect that the error caused by our use of the Zwicky magnitude is substantially smaller than 0.15 mag, which is the nominal offset calculated with the formula by Auman et al. (1989), because we have further adjusted the zero point with the accurate photometry data. So it is very unlikely that the discrepancy in H_0 can be ascribed to photometry zero-point errors. (2) Galactic extinction corrections. It may not be possible to exclude a priori the possibility that the Galactic extinction for the P-P region is much larger than that given by BH or RC2. We can see, however, that this is also unlikely: for the sample of Aaronson et al. (1986) the nominal distance moduli derived from the B -band TF relation agree with those from the H -band TF relation within less than 0.06 mag. If the extinction were large enough to account for the discrepancy, it would spoil the agreement by 0.5 mag between the TF distances with the two bands. (3) Miscorrection for the Malmquist bias. In the 4000–6000 km s⁻¹ range of the P-P region the correction for the bias is quite small for $p = 2.6$ – 2.7 and is at most 10% for $p = 2.5$ – 2.6 with the full sample, whereas the average correction is as large as 0.4 mag. The overestimation of the bias for the P-P cluster is hence little, and the present data do not seem to allow $H_0 > 80$ km s⁻¹ Mpc⁻¹. The correction for the cluster population bias is estimated to be 0.27 mag for the Coma Cluster. The matching of the two Hubble constants requires that the correction be as large as 0.75–0.95 mag. The analysis of Fukugita et al. (1991) shows that the correction could be 0.7 mag only if the sample were limited by $B_T^0 \leq 13.8$ mag (this roughly corresponds to $m_Z \leq 14.5$ mag). The samplings, however, were substantially deeper. It seems unlikely that the error of corrections alone accounts for the entire discrepancy discussed here.

The remaining possibilities are (4) that the TF relation is not universal and (5) that the P-P region (or the Coma Cluster) as a whole participates in a large-scale inward (outward) streaming, even increasing with the distance, or there is a $\sim 20\%$ anisot-

ropy in the Hubble flow. This is consistent with the claim by Willick that the Pisces-Perseus supercluster is moving toward the Local Group relative to the Coma Cluster with a velocity of 500 km s⁻¹ or more. Our data, however, indicate that this “infall motion” continues up to the distance as far as 10,000 km s⁻¹ or more. The possibility that a large-scale streaming toward the Local Group affects the region only up to $cz \sim 5000$ – 7000 km s⁻¹ is not favored in our analysis, because this requires that the net dispersion of the TF relation be as small as ≤ 0.2 mag, which does not seem to be consistent with our observation.

6. CONCLUSION

In this paper we have studied the Hubble flow in the Pisces-Perseus region with the TF relation in the B band using a nearly complete magnitude-limited sample by Giovanelli and Haynes. We have carefully examined observational selection effects in both magnitudes and velocity widths. We found that control over the Malmquist bias is essential in obtaining the correct value for the Hubble constant from magnitude-limited samples. We found that the Hubble constant from the Pisces-Perseus supercluster (referred to as the Pisces cluster by Aaronson et al. 1986) is $H_0 = 79.9 \pm 5.7_{-7.4}^{+8.9}$ km s⁻¹ Mpc⁻¹ (CMB rest frame) or $H_0 = 86.8 \pm 6.2_{-8.0}^{+9.7}$ km s⁻¹ Mpc⁻¹ (Local Group centroid). The latter value will be modified to $H_0 = 81.1$ km s⁻¹ Mpc⁻¹ ($H_0 = 81.5$) if the Virgo infall (and the local anomaly) is taken into account. While the nominal value of H_0 from the sample used by Aaronson et al. agrees well with theirs from the H -band TF relation, our small values are a consequence of the Malmquist bias. These results are insensitive to the absorption correction scheme and details of the model used to calculate the Malmquist bias, except for the magnitude of the dispersion of the TF relation, which we found to be $\sigma \sim 0.45$ – 0.5 mag inclusive of the scatter due to errors of input data. We discussed the use of the Zwicky magnitude; while the error of this has often been emphasized, it does not pose a serious problem for the analysis, provided that the zero point is calibrated carefully.

We found that the values quoted in equations (15) and (16) correctly describe the Hubble flow up to the distance $cz \sim 10,000$ km s⁻¹ or more. Our global values of H_0 are $78.5 \pm 5.5_{-7.2}^{+8.7}$ km s⁻¹ Mpc⁻¹ (CMB rest frame) and $83.2 \pm 5.8_{-7.6}^{+9.2}$ km s⁻¹ Mpc⁻¹ (Local Group centroid). No conspicuous peculiar velocity flow is detected in the region 2000 km s⁻¹ < cz < 14,000 km s⁻¹ within the sample. We detected an inflow only up to $cz = 2000$ km s⁻¹.

We noted, however, that our value of H_0 is smaller than that deduced from the Coma Cluster by 20%, which corresponds to 2 standard deviations, even if we take account of all possible systematic errors that we could detect. This suggests that either there exists a very large-scale (> 100 Mpc) peculiar velocity flow effect on the galaxies in the P-P direction, or the Hubble flow is slightly anisotropic, if the TF method is not environmentally affected and remains a good universal distance indicator.

We would like to thank Sadanori Okamura for many discussions from time to time. We also acknowledge Yoshihiro Nakai and his collaborators at the Kwasan Observatory of Kyoto University for allowing our use of the Kwasan Image Processing System, and Pekka Teerikorpi for suggesting an analysis with the variables given by equations (17) and (18). We are also grateful to Caleb Scharf for his invaluable comments improving the manuscript.

REFERENCES

- Aaronson, M., Bothun, G., Mould, J., Huchra, J., Schommer, R. A., & Cornell, M. E. 1986, *ApJ*, 302, 536
- Aaronson, M., et al. 1982, *ApJS*, 50, 241
- Aaronson, M., Mould, J., & Huchra, J. 1980, *ApJ*, 237, 655
- Auman, J. R., Hickson, P., & Fahlman, G. G. 1989, *PASP*, 101, 859 (AHF)
- Bothun, G. D., Aaronson, M., Schommer, B., Mould, J., Huchra, J., & Sullivan, W. T., III. 1985, *ApJS*, 57, 423
- Bothun, G. D., & Cornell, M. E. 1990, *AJ*, 99, 1004
- Bottinelli, L., Fouqué, P., Gouguenheim, L., Paturel, G., & Teerikorpi, P. 1987, *A&A*, 181, 1
- Bottinelli, L., Gouguenheim, L., Paturel, G., & de Vaucouleurs, G. 1980, *ApJ*, 242, L153
- Bottinelli, L., Gouguenheim, L., Paturel, G., & Teerikorpi, P. 1986, *A&A*, 156, 157
- Burstein, D., & Heiles, C. 1978, *ApJ*, 225, 40
- . 1982, *AJ*, 87, 1165
- . 1984, *ApJS*, 54, 33
- Cornell, M. E., Aaronson, M., Bothun, G., & Mould, J. 1987, *ApJS*, 64, 507
- de Vaucouleurs, G. 1977, *ApJS*, 33, 211
- de Vaucouleurs, G., de Vaucouleurs, A., & Corwin, Jr. H. G. 1976, *Second Reference Catalogue of Bright Galaxies* (Austin: Univ. Texas Press) (RC2)
- Efstathiou, G., Ellis, R. S., & Peterson, B. A. 1988, *MNRAS*, 232, 431
- Fasano, G. 1985, *A&AS*, 60, 285
- Feast, M. W. 1991, in *Observational Test of Cosmological Inflation*, ed. T. Shanks et al. (Dordrecht: Kluwer), 147
- Fouqué, P., Bottinelli, L., Gouguenheim, L., & Paturel, G. 1990, *ApJ*, 349, 1
- Freedman, W. L. 1990, *ApJ*, 355, L35
- Fukugita, M., & Ichikawa, T. 1992, in preparation
- Fukugita, M., Okamura, S., Tarusawa, K., Rood, H. J., & Williams, B. A. 1991, *ApJ*, 376, 8
- Gavazzi, G., & Trinchieri, G. 1989, *ApJ*, 342, 718
- Giovanelli, R., & Haynes, M. P. 1984, *AJ*, 89, 1
- . 1985, *AJ*, 90, 2445 (GHI)
- . 1989, *AJ*, 97, 633 (GHII)
- Giovanelli, R., Haynes, M. P., Myers, S. T., & Roth, J. 1986, *AJ*, 92, 250 (GHMR)
- Giraud, E. 1986, *ApJ*, 301, 7
- Han, M., & Mould, J. 1990, *ApJ*, 360, 448
- Haynes, M. P., & Giovanelli, R. 1984, *AJ*, 89, 758
- Hubble, E. P. 1926, *ApJ*, 64, 321
- Jacoby, G. H., Ciardullo, R., Ford, H. C., & Booth, J. 1989, *ApJ*, 344, 704
- Kodaira, K., & Watanabe, M. 1988, *AJ*, 96, 1593
- Kraan-Korteweg, R. C., Cameron, L. M., & Tammann, G. A. 1988, *ApJ*, 331, 620 (KCT)
- Kron, G. E., & Shane, C. D. 1976, *Ap&SS*, 39, 401
- Longo, G., & de Vaucouleurs, A. 1983, *A General Catalogue of Photoelectric Magnitudes and Colors in the U, B, V System* (Univ. Texas Monographs in Astronomy, No. 3) (LdV)
- Malmquist, K. G. 1922, *Medd. Lunds Astron. Obs.*, Band 16, No. 23 (No. 100)
- Mould, J., Aaronson, M., & Huchra, J. 1980, *ApJ*, 238, 458
- Nilson, P. 1973, *Uppsala General Catalogue of Galaxies* (Uppsala: Uppsala Offset Center AB) (UGC)
- Pierce, M. J., & Tully, R. B. 1988, *ApJ*, 330, 579
- Postman, M., & Geller, M. J. 1984, *ApJ*, 281, 95
- Robert, M. S. 1978, *AJ*, 83, 1026
- Rubin, V. C., Burstein, D., Ford, W. K., Jr., & Thonnard, N. 1985, *ApJ*, 289, 81
- Sandage, A. 1988, *ApJ*, 331, 605
- Sandage, A., & Tammann, G. A. 1976, *ApJ*, 210, 7
- . 1981, *A Revised Shapley-Ames Catalog of Bright Galaxies* (Washington, DC: Carnegie Institution of Washington) (RSA)
- . 1984, *Nature*, 307, 326
- Schechter, P. L. 1976, *ApJ*, 203, 297
- . 1980, *AJ*, 85, 801
- Smoot, G. F., et al. 1991, *ApJ*, 371, L1
- Tammann, G. A. 1987, in *IAU Symp. 124, Observational Cosmology*, ed. A. Hewitt & G. R. Burbidge (Dordrecht: Reidel), 151
- Teerikorpi, P. 1984, *A&A*, 141, 407
- . 1987, *A&A*, 173, 39
- Tully, R. B. 1988, *Nature*, 334, 209
- Tully, R. B., & Fisher, J. R. 1977, *A&A*, 54, 661
- van den Bergh, S., Pierce, M. J., & Tully, R. B. 1990, *ApJ*, 359, 4
- Willick, J. 1990, *ApJ*, 351, L5
- Zwicky, F., Herzog, E., Wild, P., Karpowicz, M., & Kowal, C. T. 1961–1968, *Catalogue of Galaxies and of Clusters of Galaxies* (Zürich: L. Speich) (CGCG)